Confidentiality Statement

Please note that this document contains confidential information that is proprietary to the Center for Particulate and Surfactant Systems. We expect that you will protect the confidential nature of the materials within this booklet as well as the information given during the accompanying meetings and presentations.

ULTRASMALL MULTIFUNCTIONAL SILICA NANOPARTICLES

Lisbeth Ruiz[1], James Ashbaugh[1], Megan Hahn[1], Parvesh Sharma[1], Kevin Powers[1], Stephen R. Grobmyer[2], Brij M. Moudgil[1]
[2]Department of Surgery, College of Medicine; and
[1]Particle Engineering Research Center, Department of Materials Science and Engineering, College of Engineering
University of Florida, Gainesville, Florida

Objectives: To reduce the cost of detection and/or treatment of diseases noninvasively using ultrasmall nanoparticles

Challenges: Encapsulation and retention of NIR dyes in ultrasmall silica nanoparticles; purification of particles without agglomeration

Intellectual Motivation:

- Targeting tumors with high metabolic rates is commonplace in medical imaging.
- Current technology requires expensive equipment such as PET and MRI.
- The induction of ultrasmall nanoparticles to the medical field presents a unique opportunity for:
  - Targeted drug delivery
  - Therapy (e.g., Photothermal ablation , Photodynamic therapy)
  - Diagnostics

Ultrasmall Nanoparticles Exploiting Increased Cell Metabolism

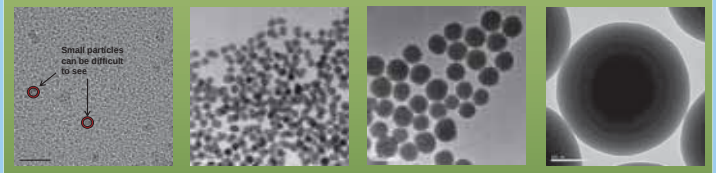

<10 nm | 30 ± 5 nm | 75 ± 5 nm | 330 ± 20 nm

Particles with NIR dye have been synthesized in various sizes

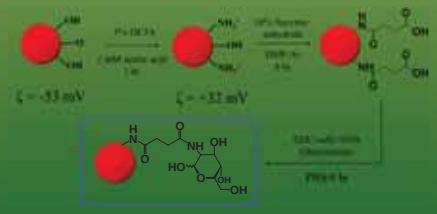

Particles <10 nm are functionalized with glucose as illustrated above

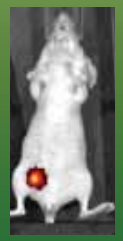

After intravenous injection of particles, a tumor can be seen in a test mouse

Irradiated Tumor Cells for Targeted Treatment with Functional Nanoparticles

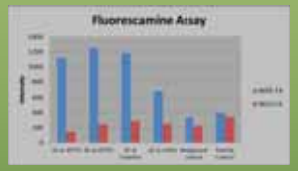

Aminosilanes were used for functionalization of the nanoparticle surface

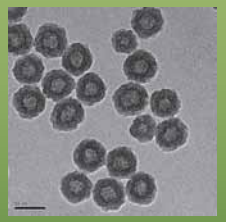

Nanoparticles with NIR dye and 43.77 mV zeta potential

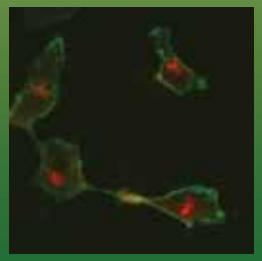

- MDA-MB-231 cancer cells have taken up NIR dye doped silica nanoparticles
- The cells have been irradiated and are no longer proliferative
- They can now be reintroduced into the subject to seek out metastases.

Industrial Relevance of Silica NPs

❖ ***Separation Processes***

Enhance the mechanical and permeation properties of membranes

❖ ***Insulation***

- Aerogels
- Synthetic porous material
- 1000 times less dense than glass
- Composed of 99.8% air and 0.2% NPs

❖ ***Catalysis***

- Large surface-to-volume ratio
- Applications range from fuel cells to catalytic converters and photocatalytic devices

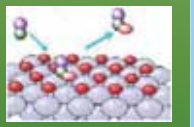

Future Work

- Imaging can be optimized by adjusting particle concentration
- Further *in vivo* testing is needed for data on autologous cell targeting
- Heat emitting dye should be tested for selective photothermal ablation

Acknowledgement: DOD/CDMRP Breast Cancer Concept Award (2010-2011): Contract # W811XWH-10-1-0883

UF UNIVERSITY of FLORIDA
The Foundation for The Gator Nation

PaSS

COLUMBIA UNIVERSITY IN THE CITY OF NEW YORK

Visible Light-Activated Transparent Antimicrobial Coatings

Wei Bai[1,2] Vijay Krishna[2], Abhinav Thakur[2,3], Ben Koopman[1, 2] , Joseph Navarro[4] and Brij Moudgil[2,3]

[1]Dept of Environmental Engineering Sciences, [2]Particle Engineering Research Center, [3]Dept of Materials Science and Engineering, University of Florida, [4]NanoHygienix LLC

1. Timeline: Concept to Product

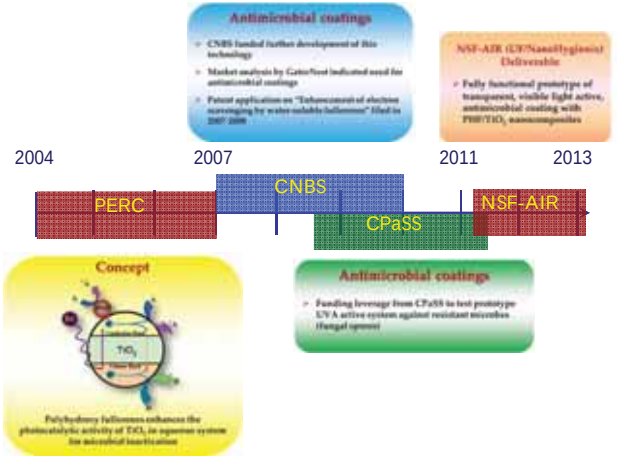

2. Product Criteria

- Transparent
- Visible light active
- Stable liquid formulation
- Compatible with commercial sprayers
- 90% of microbes (e.g., MRSA) inactivation in 12 hours (i.e., 2x faster than competition)

3. Coating Design

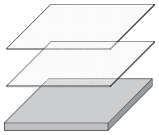

Active coating: PHF/TiO_2

Inert coating

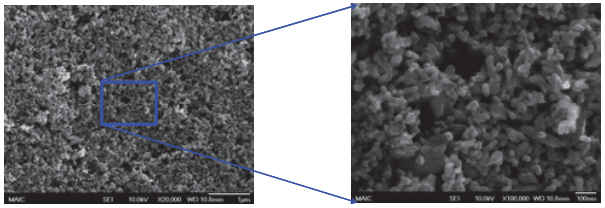

0.25 μm thickness

4. Visible Light Active Photocatalyst

- Two layer coating system:
  - Bottom coating: rutile or silica
  - Top coating: anatase or P25

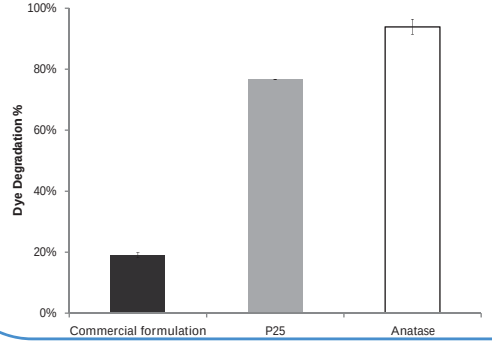

5. Stable Liquid Formulation

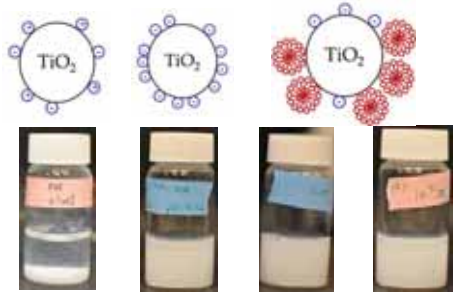

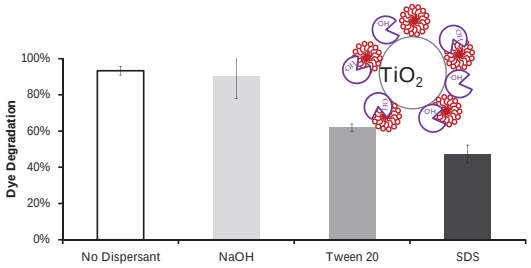

6. PERC nanocomposite kills MRSA surrogate 1.5 times faster

7. Broader Impacts and Industrial Relevance

- Removal of VOCs
- Odor control & air sanitizer
- Add-in for presently used household disinfectants

→ Kemira, Cytec, Procter & Gamble, Unilever, Church & Dwight, Evonik

- Controlled release of perfumes and other actives
- Antimicrobial coatings

→ Ecolab/Nalco, Akzo Nobel, BASF, Ashland, Johnson & Johnson, NanoHygienix

8. Timeline

Major Tasks	2011		2012				2013			
	Q3	Q4	Q1	Q2	Q3	Q4	Q1	Q2	Q3	Q4
Task 1.1: Determine optimum weight ratio of PHF/TiO_2 in the nanocomposite (UF)										
Task 1.2: Evaluate optimized PHF/TiO_2 nanocomposite for destruction of target microbes (UF)										
Task 2.1: Select system for dispersing the nanocomposite (UF)										
Task 2.2: Stage I prototype testing (UF)										
Task 2.3: Stage II prototype testing (NanoHygienix)										
Develop business plan (apply SBIR)										

UF UNIVERSITY of FLORIDA
The Foundation for The Gator Nation

PASS Acknowledgements : NSF–AIR (Grant # 1127830); CNBS; CPaSS

COLUMBIA UNIVERSITY IN THE CITY OF NEW YORK

Spring 2012 IAB Meeting – February 13-15, 2012

Effect of NaOH Concentration in Polyhydroxy Fullerene Synthesis

Eric Bidinger[1], Molly Skinner[2], Angelina Georgieva[2], Vijay Krishna[2], Ben Koopman[3], and Brij Moudgil[2]

Department of Chemical Engineering[1], Particle Engineering Research Center[2], Environmental Engineering Sciences[3], University of Florida; Gainesville, FL 32611

Objectives

- Determine the kinetics of hydroxide addition to fullerene
- Find property differences in the products made under different concentrations of NaOH

Motivation

- Understand and control the synthesis of polyhydroxy fullerenes(PHFs)

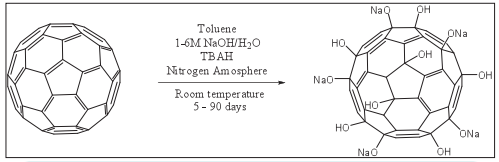

Procedure: Dissolved C_{60} in toluene in the presence of surfactant tetrabutyl ammonium hydroxide (TBAH) and added 1-6M aq.NaOH. Stirred them under nitrogen at room temperature until reaction completed. Toluene removed, water layer freeze dried, washed with cold MeOH, purified with Sephadex.

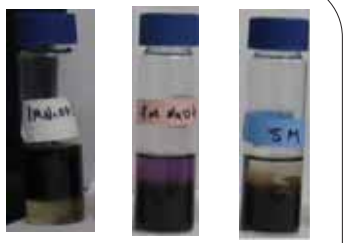

Before Reaction | During Reaction | After Completion

Industrial Relevance:

- PHFs have a wide range of applications in cosmetics, pharmaceuticals, and agriculture
- Photothermal applications can be applied to tumor therapies, or nutrient releases in agriculture
- Gadolinium PHFs can be used as a safer MRI contrasting agent

Conc. NaOH	Days to completion
19M	<1 day
6M	3 days
5M	5 days
4M	13 days
3M	20 days
2M	~120 days
1M	~180 days

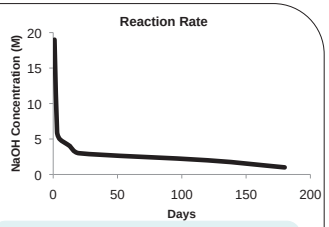

As the concentration decreases, the time needed for completion increases

FTIR Analysis

Overlapping FTIR to show similarities between different concentrations

Duplicated 6M NaOH FTIR to show reproducibility

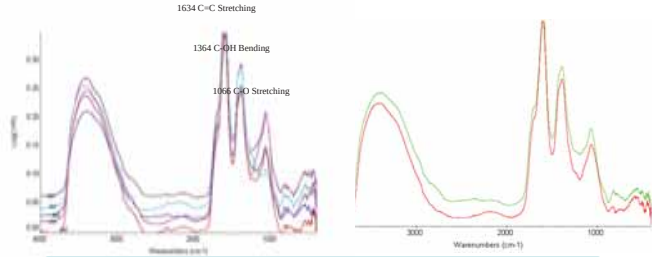

Note: these spectra are stacked, they do not all start at the origin

Heating of PHF Solution by Near IR Laser

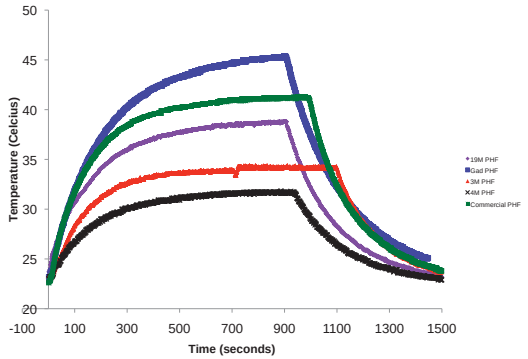

Kinetics of PHF Synthesis

.25mg/ml C_{60}, 6M NaOH

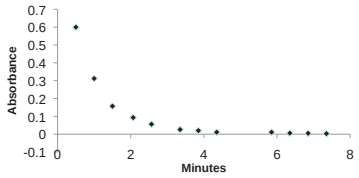

Log(Absorbance) vs Time

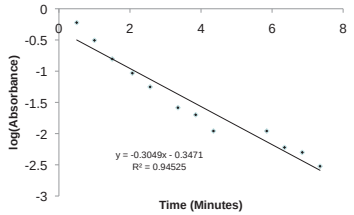

Strong correlation to logarithmic model

Sodium Removal by Sephadex

FTIR spectrum before Sephadex

Sephadex Purification

FTIR spectrum after Sephadex

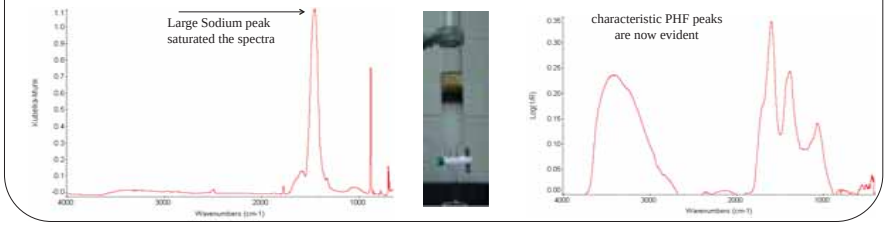

Conclusions:

- FTIR spectra are reproducible
- Heating profiles are different enough to suggest a difference in structure due to differences in OH concentration
- FTIR alone is not sufficient to characterize PHF structure

Future Plans:

- Continue experiment and model of PHF heating under near IR laser

References: 1. Li, J., Takeuchi, A., Ozawa, M., Li, X., Saigo, K. Kitazawa, K. C_{60} PHF Formation catalysed by Quaternary Ammonium Hydroxides . J. Chem. Soc., Chem Commun. 1993.

Acknowledgement: This material is based upon work supported by the National Science Foundation under Grant No. 0749481 and by the CPaSS industry members.

Prediction of Particle Charging Behavior in Gas-Solid Pipe Flow

Poom Bunchatheeravate[1], Yusuke Fuji[2], Jennifer Curtis[1], Shuji Matsusaka[2]

Department of Chemical Engineering, University of Florida; Gainesville, FL 32611 USA[1]

Department of Chemical Engineering, Kyoto University, Kyoto 615-8510, Japan[2]

Objectives: To able to predict how particles charge in a pipe flow system by doing experiments on a laboratory scale

Industrial Relevance:

The ability to control particle charge can prevent undesired effects such as clogging or explosion. Charged particles can also be used in other particle processes

Broad Appeal:

Technique can by applied to any dilute-phase pneumatic conveying process

Materials and Method

1 Feeder:
- Two piezo electric vibrators are connected to the feeder table
- Feeder controller sends electrical signal to the vibrator causing the feeder table to vibrate and feeds particle to the ejector section.
- Particle mass flow rate in the system can be control led using the feeder controller
- The particles are 52µm borosilicate spheres

2 Ejector:
- The flow in the system is driven by compressed air
- The compressed air creates suction that draws particles in from the feeder
- Flow is set at 15m/s
- Particles leaving the ejector enter into the particle charger
- ----> is the air flow path

3 Charger:
- Particle charger developed by Matsusaka et al[1]
- Voltage applied to the charger is used to control particle charge
- The initial charge of the particle can be modified before entering the pipe section

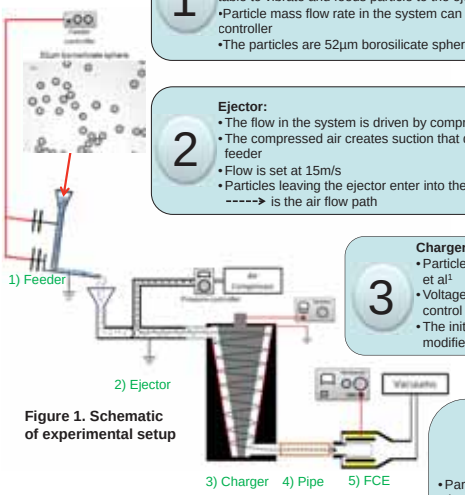

Figure 1. Schematic of experimental setup

4 Pipe:
- Particles enter a 1m straight pipe to affect the particle charging in pipe
- 2 types of pipe:
  - Copper pipe (conductor)
  - Natural glass pipe (insulator)

5 Faraday Cup Electrometer (FCE):
- Particles are pulled by vacuum into the FCE where total particle charge and total mass are measured
- The average specific charge is calculated with the units (nC/g)
- The initial charge (q_{in})and the charge after 1m pipe (q_{out})are measured at different q_{in}

Results

Borosilicate-Natural Glass Pipe

In Figure 2:
- The red line is the initial particle charge (q_{in}) vs the particle charge after 1m pipe (q_{out})
- The black line is $q_{in} = q_{out}$.

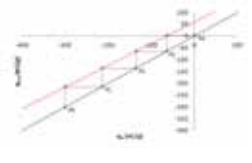

Figure 2 Qin Vs Qout relation for borosilicate-natural glass pipe

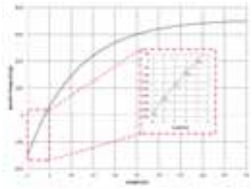

Figure 3 Charging profile for borosilicate-natural glass pipe

In Figure 2, it is possible to pick an initial particle charge (P0), and determine the particle charge at any one meter increment, this is done so by the following method
1. Find P0 in the $q_{in} = q_{out}$ line
2. Draw a vertical line from P0 to q_{in} vs q_{out} line. This point is the charge after 1m pipe length
3. Draw a horizontal line from the intersection point from step 2 to the $q_{in} = q_{out}$ line, P1.
4. Repeat step 2 and 3 for additional length increments

Figure 3 is the charging profile of borosilicate particle in natural glass pipe. It is made by plotting P0, P1, P2, P3, etc. as a function of pipe length. Note that the particle charge reaches an equilibrium after a certain length

Borosilicate-Copper Pipe

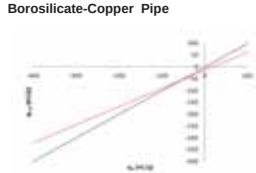

Figure 4 Qin Vs Qout relation for borosilicate-copper pipe

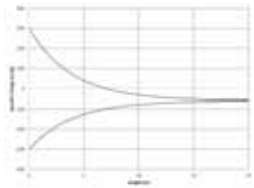

Figure 5 Charging profile for borosilicate-copper pipe

Figure 4 presents the qin vs qout plot for copper pipe. In this plot the equilibrium charge can be visualized.
Figure 5 shows the charging profile using initial particle charge of +300nC/g and -300nC/g

Validation

The results are compared with experiments measuring the same particle type in the same type of pipe. For the validating experiment, particle charges are measured with 1m, 2m, 3m, and 4m pipe. The measured charge (circle dot) are plotted together with the charging profile calculated from q_{in} vs q_{out} relationship (solid line).
Figures 6 and 7 shows the comparison for borosilicate particle in natural glass and copper pipe respectively

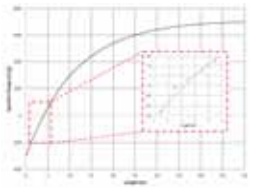

Figure 6 Plot comparing the calculate charge profile (solid line) with experimental data (dot) for borosilicate-natural glass pipe

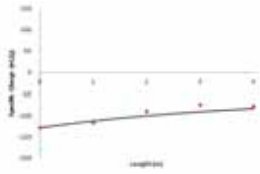

Figure 7 Plot comparing the calculate charge profile (solid line) with experimental data (dot) for borosilicate-copper pipe

Comparison with Other Study

Matsusaka et al.[2] performed particle charge measurement using different types of particles in a metal pipe. They also found that the particle charge depends on the initial charge of the particle, the length of pipe, and the equilibrium charge.
The relationship was summarized as:

$$\bar{q}_m(L) = \bar{q}_{m0} exp\left(-\frac{L}{L_q}\right) + \bar{q}_{m\infty}\left(1 - exp\left(-\frac{L}{L_q}\right)\right)$$

- L - Pipe length Particle travel through
- L_q - Characteristic length
- $\bar{q}_m(L)$ - Particle charge after L pipe length
- $\bar{q}_{m0}$ - Initial particle charge
- $\bar{q}_{m\infty}$ - Equilibrium charge of particle in the pipe

It was found that this relationship perfectly represented the charging profiles measured in the study. The characteristic lengths are 11.32m and 3.87m for borosilicate particles in natural glass pipe and copper pipe respectively.

Acknowledgement

The author would like to acknowledge NSF PIRE program (NSF OISE 0968313)

Future Works

- Using a CFD model to predict impact frequency in the pipe flow
- Determine the charging relationship as a function of particle collisions

Reference

1. Matsusaka S, Ando K, Tanaka Y; Development of electrostatic charge controller for particle in gasses using centrifugal contact. J Soc Powder Technol. 2008, vol. 45, p380-386
2. Matsuska S, Oki M, Masuda H; Control of electrostatic charge on particles by impact charging. Adv Powder Technol 2007. vol. 18 no 2, p229-244

UF UNIVERSITY of FLORIDA
The Foundation for The Gator Nation

PaSS

COLUMBIA UNIVERSITY IN THE CITY OF NEW YORK

Enzyme Enhancement via Interactions with Surfactants

Michael Chin, P. Somasundaran

Columbia University: Fu School of Engineering; New York, NY 10027

Objectives: Explore mechanism behind synergistic enzyme-detergent behavior

Challenges: Exploring changes in protein structures and function due to surfactant

Intellectual Motivation: A more detailed understanding of protein structure function, conformation and dynamics in colloid systems previously unexplored

Industrial Relevance: More effective application of enzymes in detergent formulations, lowering costs and opening pathways to "Greener" enzyme based products

Broad Appeal: Implications in any application involving functional proteins in colloid environment. i.e. bio-solar, vaccine formulation, bio-fuels

Methods:

- Enzyme Kinetics
  - ➢ Measure "functionality" of enzymes in different solution
- Life Time Fluorescence
  - ➢ Probe flexibility of local environments
- Surface Tension
  - ➢ Measure colloid propertiees of protein surfactant mixtures
- ESR / NMR
  - ➢ Detailed measurement of specific structure movement

A

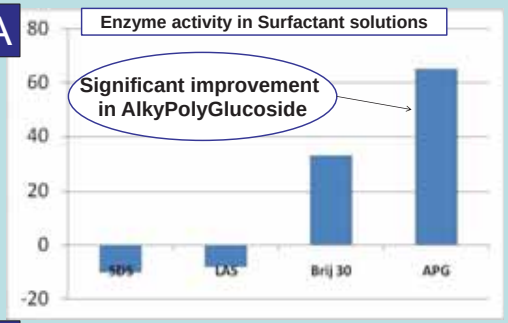

B

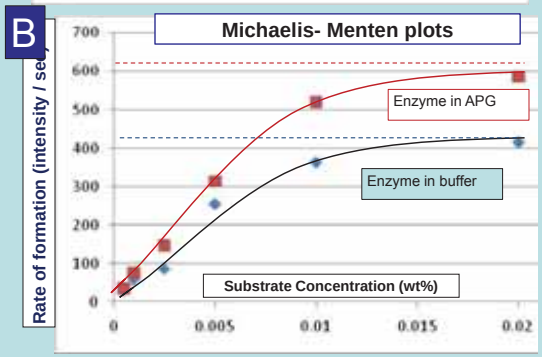

a) Initial activity tests showed that enzyme in non-ionic surfactants like APG yielded MORE product than when in buffer alone

b) Kinetics studies indicated a higher max reaction rate and thus greater catalytic rate constant

c) Comparison between APG concentration and protease catalytic rate reveals link between CMC and enhancement

d) Time dependent fluorescence : Enzyme active site more flexible in Brij-30 solution

C

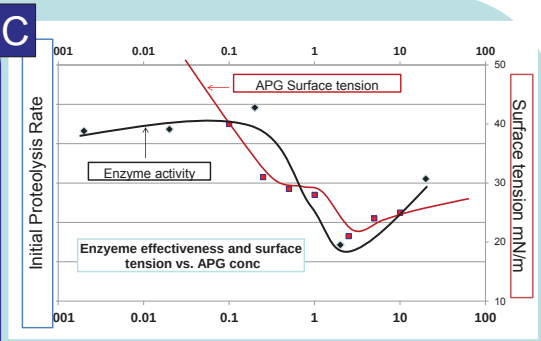

D

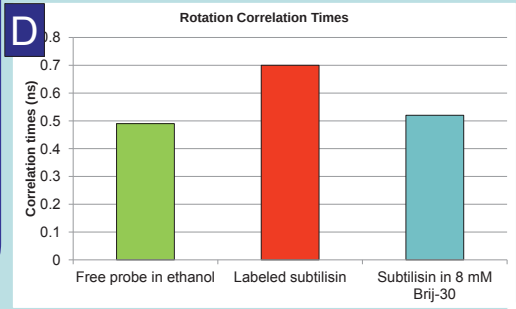

Summary and Impact: Through kinetics, surface tension and anisotropic fluorescence decay we are beginning to establish structure dynamics as a primary mechanism enabling surfactants to affect enzyme function - Improving enzymes through surfactant selection

Acknowledgement: This material is based upon work supported by the National Science Foundation under Grant No. 0749481 and by the CPaSS industry members

Biological Uptake of Polyhydroxy fullerenes in the Aquatic Environment

Angelina Georgieva[1], Eric Bidinger[2], Vijay Krishna[1], Jie Gao[3], Jacquelyn Knapik[3], David Barber[4], Ben Koopman[3], Brij Moudgil[1]

Particle Engineering Research Center[1], Department of Chemical Engineering[2], Department of Environmental Engineering Sciences[3], Department of Pathology [3], Center for Environmental and Human Toxicology[4], University of Florida; Gainesville, FL 32611

Introduction

Exposure to chemicals in the environment can lead to adverse effects on the health of living organisms, from subtle biochemical changes to disease and death. Fullerenes and polyhydroxy fullerenes (PHF) are widely explored for biomedical applications but there is limited information regarding their biocompatibility. Presented were already first evidences of their therapeutic applications. PHFs synthesized in our lab are fully water soluble derivatives of fullerenes with possible medical applications such as photoacoustic imaging. In the present work their environmental fate and their uptake by aquatic organisms *Daphnia Pulex* (water fleas) and *Danio Rerio* (Zebrafish) were studied.

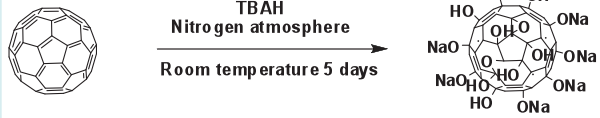

Scheme 1. Synthesis Procedure for fullerene's phase transition into water layer

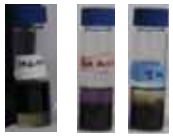

Phase transition of C60 from oil layer to water layer

Industrial Relevance

Toxicological model study: Environmentally benign nanoparticles of PHF with possible therapeutic effects and photoacoustic imaging qualities were subject to test.

Intellectual Motivation for Research:
Increased contrast of photoacoustic signal and decrease of mouse tumor by 72% for area treated with PHF.

- Water fleas were exposed to varying concentrations of PHF up to 20mg/L over 8 days
- No casualties were observed.

Results from Daphnia pulex (water fleas) Exposure to PHF

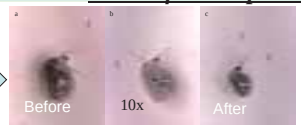

Microscopic images of daphnids exposed to (a) control, (b) .001 mg/L of PHF, and (c) 20 mg/L of PHF after 2 days.

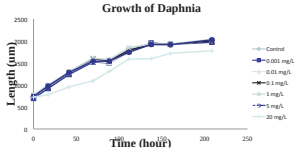

Body lengths of tested daphnids over a duration of 8 days

Toxicological results: No acute toxicity; Extended life span and stimulated reproduction up to 20mg/L of PHF.

Results from Danio Rerio (Zebrafish) Exposure to PHF

Neonates and adult Zebrafish were exposed to varying concentrations of PHF– pictures and histological images were analyzed; ~50 total fish were tested, one casualty in 150 mg/L of a neonate.

Toxicological result: No acute toxicity; Surviving of Zebrafish neonates in 150mg/L of PHF and adults in 500mg/L of PHF

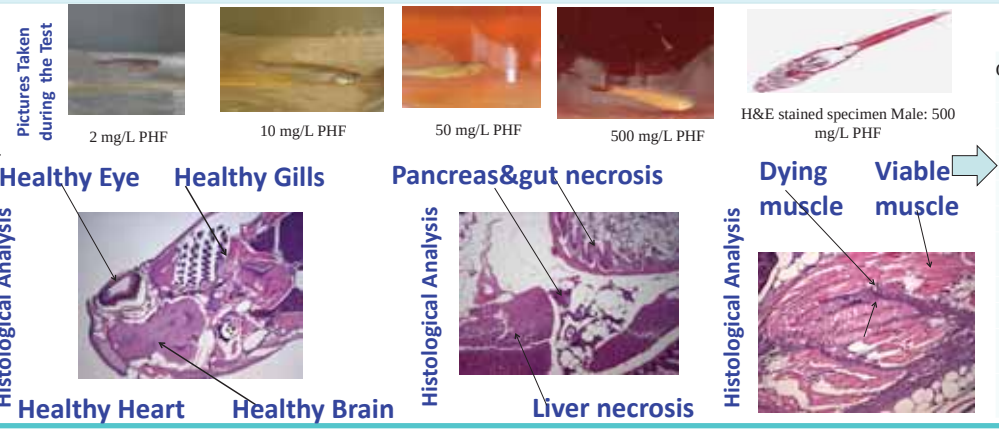

Table 1. H&E Histological analysis results

Concentration PHF (mg/L)	Necrosis	Inflamation	Autolysis
Control A	No	No	Gut & liver
2A	Muscle	Mild	Gut
10A	Focal Muscle	Mild	Gut & liver
50A	No	Mild	Gut & liver
500A1	No	Mild	Gut
500A2	Focal Muscle	Mild	Gut, Liver&Pancreas
500B1	No	Mild	Gut
500B2	No	Mild	Gut
500C1	Multifocal Muscle	Mild	Gut, Liver&Pancreas
500C2	Focal Muscle	Mild	Gut, Liver&Pancreas

Summary

- *Daphnia Pulex* (water fleas) showed increased life span and stimulated reproduction 38% in 20mg/L of PHF.
- *Danio Rerio* (Zebrafish), neonates, survived exposure to PHF and no cranial and spinal malformation were noticed in neonates up to the studied 150mg/l exposure. *Danio Rerio* (Zebrafish), adult, survived extended exposure to PHF up to 500mg/L with healthy brain, gills, heart and eyes. In the highest concentration necrosis and inflammation were observed in the focal muscle, gut, liver and pancreas in some cases.

Future Work

- Compare PHF effect to other dark liquids effect like Coffee or Coca-Cola on Zebrafish.
- Further research to confirm the toxicity effects and publication of our results.

Spring 2012 IAB Meeting, February 13-15 2012

Acknowledgement: This material is based upon work supported by the National Science Foundation under Grant No. 0749481 and by the CPaSS industry members.

Fundamental Research Program Proposal: Foaming and Frothing Behavior of Green Surfactants and Fine Particulate Systems

Jun Wu, Irina Chernyshova and Ponisseril Somasundaran, Columbia University, New York, NY 10027
Angelina Georgieva, Aarthi Narayanan, Parvesh Sharma, and Brij Moudgil, University of Florida, Gainesville, FL 32611
Center for Particulate & Surfactant Systems (CPaSS)

Intellectual Motivation: Fundamental research exploring foaming/defoaming properties of green surfactants and fine particles. Understand antagonistic and synergistic effects of hydrophobically modified fine particles and green surfactant formulations.

Market Motivation:

- The US market for defoamers gravitates increasingly toward silicone and water-based.
- Use of fats and oils constitute a significant segment of overall demand.
- Increasing oil prices and environmental regulations signify the importance of developing renewable resources based foaming and defoaming modalities.

Industrial Relevance: Global market for surfactants is forecast to reach $17.9 Billion by 2015[1] with ever-stricter regulations out of environmental consideration; 1) Increased market demand 5.3% per year for environmentally friendly defoamers up to $2.77 billion total in 2015[2];

Broader Appeal: Foaming/defoaming formulations have important applications in mineral separations, detergency, boilers, paper, petroleum, paints, coating industry, biochemical separation, cosmetics, household industry and environmental remediation industries.

Definitions: Foams are gas-liquid disperse systems, stabilized by the surface elasticity and surface viscosity of the liquid films. Froths are three-phase disperse systems – gas-liquid-solid. Defoamer is insoluble in the foaming medium and has surface active properties that promote coalescence of foam. Fine particles are known to strongly influence frothing characteristics, such as froth stability, froth viscosity and gas hold-up.

Foaming power is desirable criteria of quality in many industries:

- food industries like beer, ice cream and cappuccino beverage production,
- Firefighting industries
- Household products (laundry detergents, dishwashing soaps)

Foaming power is detrimental for:

- Paper Industries
- Food Industries
- Petroleum industries
- Paint and coating industries
- Cement industry
- Waste treatment industries.

Foaming can cause leaky seals, pressure release, reduction of pump efficiency, bacterial growth, imperfection of the product, leading to rejection.

Systems:

- Sugar based and amino acid based green surfactants.
- Fine particulate systems of silica (SiO_2), kaolinite [$Al_2Si_2O_5(OH)_4$], calcite ($CaCO_3$), hydroxyapatites [$Ca_{10}(PO_4)_6(OH)_2$] and ferric (hydr)oxides [$Fe_{10}O_{14}(OH)_2$]

Green surfactants dodecyl maltoside & sodium dodecyl glutamate

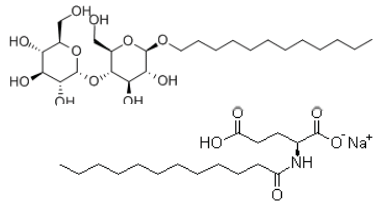

Silica (left) & ferric hydroxide (right) nanoparticles

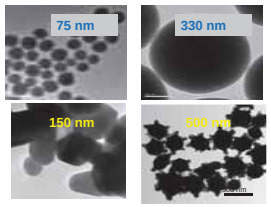

Methods: Characterization of particles size by colloidal dynamics acoustosizer and dynamic light scattering; Measuring zeta potential; Macroscopic measurements of foam/ froth stability; Vibrational Spectroscopic Studies; Computational simulation.

Deliverables: New fundamental knowledge to assist in developing foaming/defoaming formulations and theoretical models for the industries.

References: 1. Global Industry Analyst, Inc. : Surface Active Agents: A Global Strategic Business Report, 2010
2. BizAcumen, Inc.: Defoamers – World Market Review, 2010

SCANNING PROBE MICROSCOPIES: MINIATURE DETECTIVES

Megan A. Hahn, Yakov Rabinovich, Kevin Powers, and Brij M. Moudgil

Particle Engineering Research Center, University of Florida; Gainesville, FL 32611

Industrial Relevance: Surface chemistry lies at the heart of numerous industrial processes, helping to create everyday products (e.g., chemicals, fuels, electronics). Studying the interface allows researchers to elucidate atomic or molecular interactions for creating improved coatings and more efficient and/or selective processes. SPMs are major players in the study of behavior at the nm scale, and with current technology constantly getting smaller, they are poised to make even bigger impacts.

Interfacial Phenomena

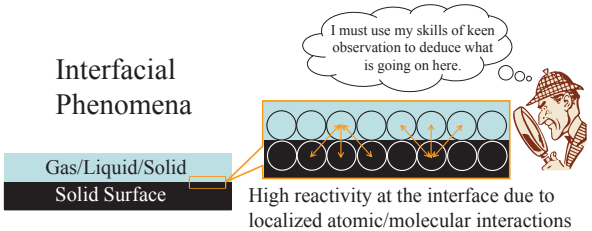

High reactivity at the interface due to localized atomic/molecular interactions

Asylum Research MFP-3D-BIO™

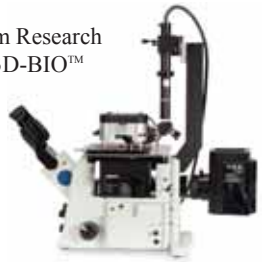

Principle of Operation

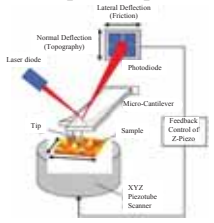

Pishkenari et al. *Chaos, Solitons & Fractals* **2008,** *37*, 748–762.

*World market revenues for SPMs in 2010 was approximately US$660 million. Industrial uses for SPMs include quality analysis and product monitoring during manufacturing processes to improve yields or reduce costs.
Report: *The World Market for Scanning Probe Microscopes*, Future Markets, Inc., July 2011.

*Instrument available for use by all CPaSS members

Modes: Contact mode; AC mode with Q-control; AFM Phase; exclusive Dual AC mode; LFM; EFM; MFM; SKPM; STM; piezoresponse force microscopy (PFM) including vector and switching spectroscopy PFM; Conductive AFM (CAFM) with ORCA module; Dual AC Resonance Tracking (DART); MicroAngelo™ nanolithography and nanomanipulation, nanoindentation.
Scan Dimensions: 90 µm × 90 µm area (0.5 nm resolution); 15 µm height (0.25 nm resolution)
Media: Air, fluid (closed fluid cell), 20-80% relative humidity, ambient to 80 °C
Forces: pN-nN range (dependent on tip, spring constant); force maps 384 × 384 points
SKPM: mV range (dependent on tip, tip-sample distance, spring constant)

CMP/Milling/Grinding

Characterization of abrasive particles or the resulting product

*Pharmaceutical ingredients
*Wafers
*Slurry particles
*Milling media
*Roughness
*Interparticle forces

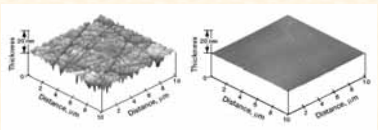

Atomic Force Microscope images of SiC wafers. Left: As-received wafer. Right: Wafer after CMP.
http://www.grc.nasa.gov/WWW/RT/RT1997/5000/5510powell.htm

AFM Imaging and Force Microscopy

Particle – Particle Image: **Interacting geometries**

Particle – Particle Image: **Adhesion force map**

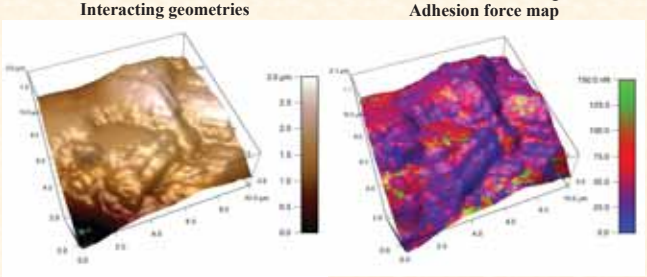

Interactions between two lunar simulant particles.
Left: Topography. Right: Adhesion force map. **(PERC)**

Emulsion and Surfactant Technology

Forces at solid/liquid or liquid/liquid interface

*Cosmetics and consumer products
*Coatings
*Corrosion inhibitors
*Oil recovery
*Mineral flotation

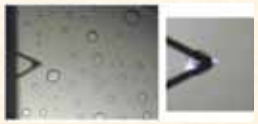

Force Curves and Microscopy

Interaction between emulsion droplets inside a polymer solution

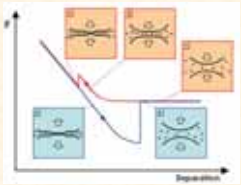

1. When the droplet surfaces are far apart they don't interact.
2. As the droplet surfaces come sufficiently close together, they start to deform; polymers remain in the thin liquid film between them.
3. As the polymers diffuse away from a region of the film, a „jump in' effect occurs which corresponds to the formation of a black spot; i.e. the local lamella thickness has reached the dimension of common black films.
4. The black spot expands with time and it keeps expanding even as the droplets are pulled apart, until a „snap out' is observed which corresponds to the droplets being suddenly disconnected.
5. After the droplets have been separated, the droplet surfaces recover their initial shape.

Axel Gromer and A. Patrick Gunning (http://www.asylumresearch.com/Applications/OilDroplets/OilDroplets.shtml)

Semiconductor Industry

Electrical device characterization

*Defect/doping levels in thin films
*Electrical junctions and heterostructures
*Transistors and integrated circuits
*Photovoltaics and solar cells
*Batteries and energy storage

Electrostatic Force Microscopy
Scanning Kelvin Probe Microscopy

http://www.mpip-mainz.mpg.de/symposium/spm2011/poster.php

Corrosion Science

Properties and effects of corrosion inhibitors

*Normal and lateral (shear) forces on surfactant/polymer layer
*Localized defects under protective layer of surfactant/polymer

http://www.paintsquare.com/news/?fuseaction=view&id=6256

Force Curves and Microscopy

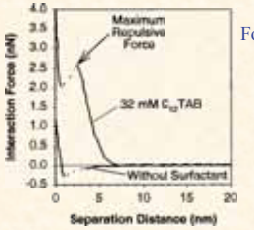

Force needed to penetrate micelle layer **(PERC)**

Measured interaction forces between the AFM tip and a mica surface in 0.1 M NaCl solution at pH 4, both with and without 32 mM of C_{12}TAB surfactant. Dotted line indicates the region of mechanical instability where the cantilever "jumps" into contact with the surface.

Adler et al. *Langmuir*, **2000,** *16*, 7255–7262.

Scanning Kelvin Probe Microscopy

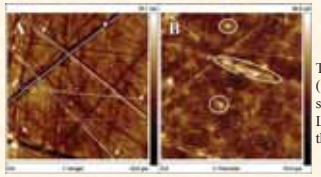

SKPM measures the work function of a surface, elucidating the local electronic structure.

Topography (A) and surface potential (SKPFM) (B) images obtained on an AISI 316 sample oxidized at T_{ox} = 423 K (t_{ox} = 15 nm). Lift height: 100 nm; Applied AC voltage on the tip: 6 V.

Maachi et al. *Corrosion Sci.* **2011,** *53*, 984-991.

Effects of thermally oxidized stainless steel

Acknowledgement: This material is based upon work supported by the National Science Foundation under Grant No. 0749481, by the CPaSS industry members, and by the State of Florida Space Related Research Initiatives Award No. 20040028/20040027.

UF UNIVERSITY of FLORIDA
The Foundation for The Gator Nation

CPaSS

COLUMBIA UNIVERSITY IN THE CITY OF NEW YORK

Spring 2012 IAB Meeting – February 13-15, 2012

Nanoparticle Suspensions: Turbidity, Surface Charge and Aggregation

S. Murthy Khandrika and P. Somasundaran
Columbia University, New York, NY 10027

The engineered NANOPARTICLES compared with natural particles to determine their transport, aggregation, stability, and fate in soil, water, and air

Physico-chemical properties of nanoparticles (NP) in the presence of minerals present in soil studied.

Goal: Understand physicochemical interactions of nanoparticles & minerals and relate to fate and transport

ZnO-kaolinite system

Key Hypothesis

- There are specific, quantifiable physicochemical properties of NMs that determine their behavior in the environment
- Intrinsic NM properties dictate their thermodynamic stability and initial interactions with suspending media
- These media interactions lead to a modification of interfacial properties at the NM surface
- This in turn, determines subsequent nano–bio/geo interfacial interactions in the environment
- The ultimate fate of NMs is governed by these interactions with environmental interfaces

NM: Nanomaterials

Ref. CEIN, UCLA proposal

Surface properties and interfacial chemistry of NMs

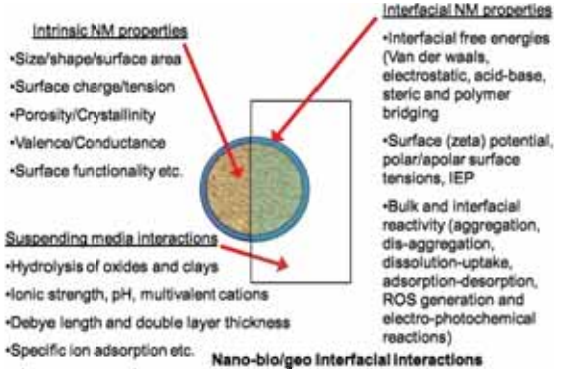

Ref. CEIN, UCLA proposal

Nanoparticles

- **Naturally occurring**
- **Anthropogenic**
- **Engineered nanoparticles**

Christopher Chang, The immune effects of naturally occurring and synthetic nanoparticles, Journal of Autoimmunity 34 (2010) J220–J243

Naturally occurring: Volcanic Ash

Ash particle, 1980 Mount St. Helens eruption, magnified 200 times

Volcanic ash: Size can be less than 1 micron

http://upload.wikimedia.org/wikipedia/commons/thumb/a/a7/MSH80_st_helens_eruption_plume_07-22-80.jpg/d11px-MSH80_st_helens_eruption_plume_07-22-80.jpg

http://volcanoes.usgs.gov/ash/images/ashem_small.jpg

Anthropogenic: Diesel exhaust particles

Diesel exhaust particles, 100nm

http://en.wikipedia.org/wiki/Diesel_exhaust

Engineered nanoparticles: ZnO, ceria, anatase etc.

ZnO 30nm suspension pH and conductivity w/ and w/o kaolinite

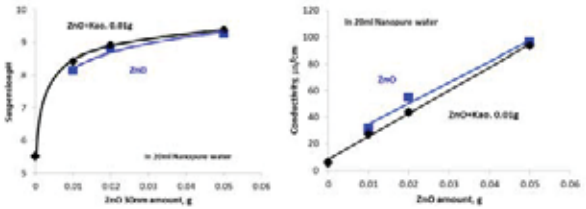

Change in pH and conductivity due to particle dissolution

Turbidity of ZnO 30nm and kaolinite particles

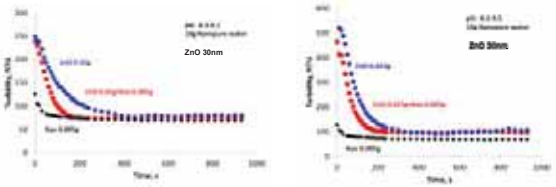

Suspensions settle faster in the presence of kaolinite. pH environmentally relevant.

Zeta potential of ZnO 30nm suspensions w/ and w/o kaolinite

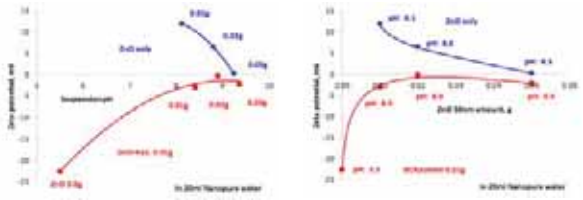

ZnO, IEP at pH: 9.5 from literature

Particle dissolution caused changes in pH and zeta potential

Particle size of ZnO 30nm suspensions w/ and w/o kaolinite

The true size of the particles in suspension

Information on particle sizes from literature

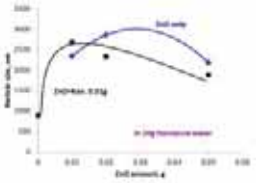

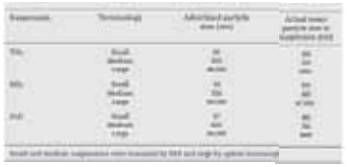

Laura K. Adams, Delina Y. Lyon, Pedro J.J. Alvarez, "Comparative eco-toxicity of nanoscale TiO2, SiO2, and ZnO water suspensions", Water Research 40 (2006) 3527–3532

Particle agglomeration noticed in suspensions

Summary

- ZnO suspensions settle faster in the presence of kaolinite. And pH Conditions are environmentally relevant.
- Zeta potential of ZnO and ZnO+kaolinite suspensions approached zero mV close to a pH of 9.5 with increasing amount of ZnO and this could be due to particle dissolution.
- Isoelectric point (IEP) of ZnO is at a pH of 9.5 from literature and corresponds to these results closely.
- Particle agglomeration in ZnO 30nm suspensions noticed with and without kaolinite.

These findings help us understand the implications of nanoparticles in the environment with regards to their interaction with minerals present in soil.

Future Plan

- Characterization of nanoparticle suspensions
- Studies with nanoparticles and other minerals
- Effect of natural organic matter on nanoparticle suspensions

Two-Fluid Modeling and Variable Gravity Experiments of Cratering of a Particle Bed by a Subsonic Turbulent Jet

Casey Q. LaMarche[1], Dr. Aldo Benividas Muran[2], Dr. Berend van Wachem[3], Dr. Peter Liever[4], and Prof. Jennifer S. Curtis[1]

Chemical Engineering Department, University of Florida, Gainesville, Fl 32611[1], Multiphase Flow Group, Chalmers University, Sweden[2], Department of Mechanical Engineering, Imperial College, England[3], Research Corporation, Huntsville, AL 35811[4]

Motivation

A multiphase continuum model that can accurately predict the interaction of a high speed fluid jet with a dense particle bed. The dense phase fluid/solids interaction model will be used to help predict the high velocity spray created during ascent and descent of lunar space crafts.

Introduction

- The lunar soil surface is covered by a thick layer of granular material (dust, rocks, etc.)
- High velocity particle spray due to the interaction of the impinging rocket plume with the lunar soil surface during the decent and ascent of lunar spacecraft.
- Impinging rocket plume on lunar surface produces ground jet that moves radially and laterally away from the jet stagnation region
- Interaction of rocket plume with the lunar surface causes particle liberation and regolith erosion: extremely hazardous particle spray.
- Scientists[1] estimate eroded particles velocities > 100 m/s
- Accurate and robust modeling of rocket exhaust interaction with the lunar surface paramount to future space exploration

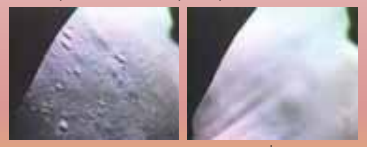

a b

Snap shots from an Apollo landing on the moon[2]. Image b haziness high velocity particle spray induced by the interaction of the lunar modules rockets with the lunar surface.

Figures of gas particle bed interactions that lead to hazardous particle ejections and could benefit from continuum modeling; (from left to bottom right) artist rendering of the particle spray ejected during space craft descent[2], Helicopter brown out[3], and saltation causing the take over of a city[4].

Experimental Data of Cratering Behavior[5]

- Experimental parametric study cratering behavior due to a gas jet
- Subsonic turbulent jet directed downward into a particle bed
- Particle bed beach sand sieved to 100-180μm
- The jet bisected by clear window crater evolution monitored by high resolution video and crater data extracted with surface tracking techniques.
- The effects of jet velocity, diameter, height above bed, density and viscosity were explored.

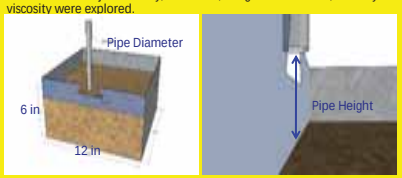

Industrial Applications

CFD modeling is a tool that can help increase efficiency by predicting better reactor or storage design, experimental insight

CFD modeling has the ability to model large scale systems, which is necessary for industrial applications.

Dense phase particle flows are prevalent in industry

CFD has and can be used to improve the performance of multiphase flow technologies

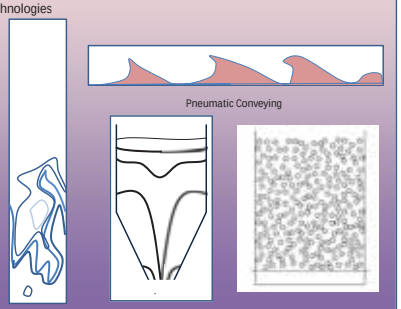

EXPERIMENT MEASURABLES

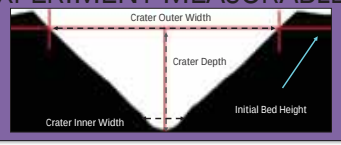

VARIABLE G EXPERIMENTS

- Cratering in Earth gravity (gee), lunar gravity, and 2-gees.
- Experiments performed with spherical particles
- Investigate effects of particle density and gravity on crater formation

Experimental set up

Experimental team in Zero G plane

CFD MODELING APPROACH

- Two fluid model: separate mass, momentum balances for each phase
- Balance of kinetic energy associated with particle velocity fluctuations
- Solid phase stress – summation of kinetic, collisional and frictional contributions
- Implementation in Fluent
- Magnitude of frictional stress greatly affects cratering behavior

FRICTIONAL MODEL

$$\overline{\overline{P}}_{s,f} = P_{s,f}\,\overline{\overline{I}} + \mu_{s,f}\left[\nabla\vec{v}_s + (\nabla\vec{v}_s)^T\right]$$

For $\varepsilon_s > \varepsilon_{s,\min}$

Frictional Pressure

$$P_{s,f} = \begin{cases} Fr\,\dfrac{(\varepsilon_s - \varepsilon_{s,\min})^n}{(\varepsilon_{s,\max} - \varepsilon_s)^p} & \varepsilon_s > \varepsilon_{s,\min} \\ 0 & \varepsilon_s \le \varepsilon_{s,\min} \end{cases}$$

Frictional Viscosity[12]

$$\mu_{s,f} = \frac{P_{s,f}\sin\phi}{2\sqrt{I_{2D}}}$$

SIMULATION DOMAIN

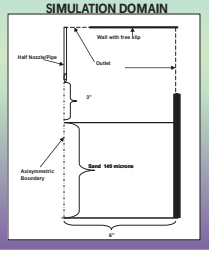

MODEL PREDICTIONS OF CRATERING

Simulated and Experimental Parametric Study
Johnson and Jackson[11] Frictional Model: Fr = 0.05, n=2, p=5

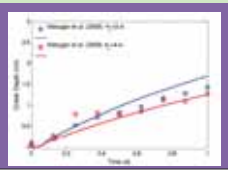

•Effect of Jet Height
•Scales ~ $1/H_p$

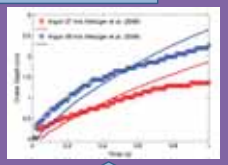

•Effect of Jet Density/ Viscosity
•Scales with ~ $\frac{\rho_p - \rho_g}{U_r^2}$ (LM)

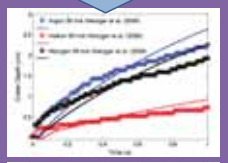

Experimental image of crater and solids volume fraction contour plot

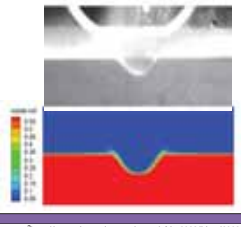

•Effect of Jet Velocity •Scales ~ Re

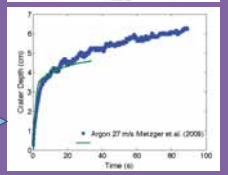

•Long time simulation prediction

CRATERING IN VARIABLE GRAVITY

Cratering polystyrene 150-300 microns

Crater depth more sensitive to jet Re ↑ as gee ↓

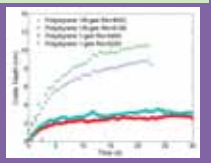

Re = 6590, 1/6-gee

t = 22 sec

Re = 6530, 1-gee

t = 22 sec

Cratering glass 150-300 microns

Crater depth ↓ as gee ↑

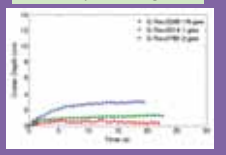

Crater inner and outer width ↓ as gee ↑

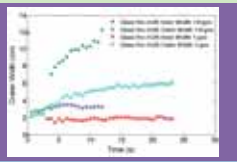

Cratering glass and polystyrene 150-300 microns in 1/6-gee

Cratering of polystyrene much more sensitive than glass to increased jet velocity

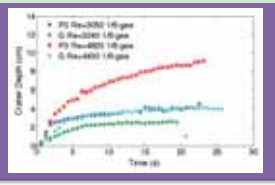

Inner crater glass width = overall crater width polystyrene

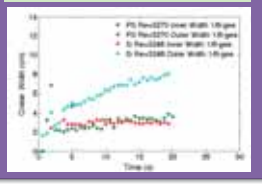

CONCLUSIONS

- The two-fluid fundamental CFD model (with the appropriate frictional stress model) is capable of predicting the salient features of the particle cratering behavior via impinging jet.
- A scaling analysis based on the governing equations in the model can describe the trends in the experimental data
- Lower density particles crater much faster and produce a larger crater.
- Cratering rate increases with decreasing gravity and the crater is larger in lower gravity.
- Dominating cratering mechanism can change based on gravity

FUTURE PLANS

- Cratering in lunar gravity and 2xEarth gravity: modeling
- Investigate cratering of lunar soil simulants and nonspherical particles: experimental and modeling
- "Multi-scale" modeling to particle phase stress to incorporate particle shape

ACKNOWLEDGEMENTS

NASA – STTR, NASA-Kennedy Space Center, Dr. Philip Metzger, Dr. Christopher Immer
Jennifer Lester
Kala Galvich

Founding provided by NASA-STTR and PIRE-NSF

References: [1]Jaffe, L. D., *SP-284, NASA, Washington DC, (1972)* 94-96., [2]*Provided by NASA: Lunar landing images and NASA Artist Concepts* .. [3]http://www.airsquadron.org/pages/africa2002/hires/2002-04-20_01%20Nouakchott.jpg., [4]http://www.defenseindustrydaily.com/V-22-Osprey-A-Flying-Shame-04822/., [5]Metzger *et al., J. Aero. Eng.*, **22**, *24 (2009)*., [6]Metzger, Private Communication (2009)., [7]Anderson and Jackson, *In. Eng. Chem. Fund.*, **33**, 1439 (1967)., [8]Jackson, *Chem. Eng. Sci.*, **52**, 2457 (1997)., [9]Jackson, *Chem. Eng. Sci.*, **53**, 1955 (1998)., [10]Lun et al., *J. Fluid Mech.*, **140**, 223 (1984)., [11]Johnson and Jackson, *JFM*. 176, 67 (1990)., [12]Schaeffer, *J. Diff. Eq.*, **66**, 19 (1987)., [13]Ocone *et. al.* AIChE Journal, **39**, 1261 (1993).

UF UNIVERSITY of FLORIDA
The Foundation for The Gator Nation

PSAS

Spring 2012 IAB Meeting – February 13-15, 2012

COLUMBIA UNIVERSITY IN THE CITY OF NEW YORK

Detailed Measurement of Particle-Laden Flows Using Laser Doppler Velocimetry

Sarah E. Mena, Zhelun Li and Jennifer Sinclair Curtis

University of Florida, Department of Chemical Engineering, Gainesville, FL, 32611

Background

Two-phase flows are prevalent across a diverse range of industrial and geophysical processes including fluidized bed reactors, pneumatic and hydraulic conveyors, and sedimentation units.

The presence of a second phase has an effect on the momentum, heat and mass transport properties of the flow. Knowledge of the behavior of two-phase flows is required for the development of accurate transport models that will help reduce problems with settled/stationary particles, improve the design of new slurry lines, and help determine optimum operating conditions in existing lines.

Particle Flow Classification

Fluid particle flows can be categorized in two regimes:

Viscosity dominated regime	Inertia dominated regime
Momentum and energy transfer occur through the fluid	Momentum and energy transfer occur by direct interaction between particles without being affected by the fluid.
Systems where the two phases have very similar densities, small particles size and low flow rates are expected to be viscosity dominated flows.	Systems with large particles and where the particles have a greater density than the fluid are expected to be inertia dominated flows.
Typical examples: Gas-solid and liquid-solid flows with small particles.	**Typical examples:** Gas-solid flows with larger and denser particles.

A method to quantify the response of particles to fluid fluctuations is the Stokes number, defined as:

$$St = \frac{particle\ response\ time}{fluid\ response\ time} = \frac{U_f \cdot \rho_s \cdot d^2}{18 \cdot \mu \cdot D}$$

Where:
Uf is the fluid velocity, ρ_s is the particle density, d is the particle diameter, μ is the fluid viscosity and D the characteristic length. The convention to classify flows is approximately:

St < 1 **Viscosity dominated**

St > 1 **Inertia dominated**

Particle Flow Responsiveness

Depending on the particles response to fluctuations in the fluid, particle fluid interaction can be seen as depicted in figure 1: two extreme behaviors of responsiveness and non-responsiveness with an intermediate region in between.

Stokes Numbers <1 **Stokes Numbers ~5-30** **Stokes Numbers >40**

Figure 1 Schematic of particle response at different Stokes numbers.
Fluid trajectory **Particle trajectory**

There is a lack of experimental data for the viscous-dominated (Stokes <~1) and transitional regime (Stokes ~5-30).

Research Objectives

Perform a systematic investigation of the effects of Reynolds number, particle size and particle concentration on the transport profiles for both the fluid and particle phase. This will include measurement of mean and fluctuating velocities of both phases at varying flow rates for viscous-dominated and transitional regimes systems.

Research Methods

A unique pilot flow facility was constructed and is fully functional for the investigation of turbulent two-phase flows.

The equipment, depicted in Figure 2, can accommodate a wide range of flow rates, particle sizes and concentrations.

The system selected for the study is water at room temperature as the fluid and glass spheres as the particles.

Flow data will be acquire using non-intrusive laser Doppler velocimetry (LDV) technique. LDV is high resolution laser based technique that can be used to obtain instantaneous and averaged velocity measurements. LDV is one of the most popular methods for the measurement of local velocity.

Experimental Facility

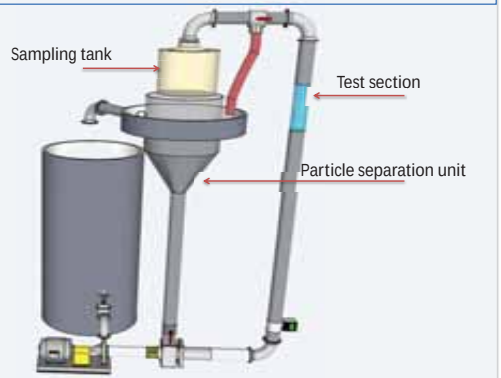

Figure 2 Diagram of the pilot scale slurry facility

For high solid concentrations the index of refraction between the fluid and the particles will be match to allow velocity measurements with LDV. Early tests for Pyrex glass and silica gel particles using a concentrated solution of sodium iodide were conducted showing encouraging results. Pictures for some tests are shown in Figure 3.

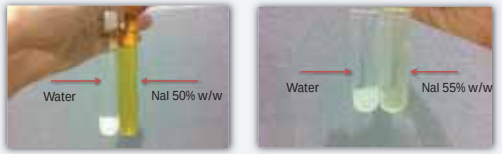

Figure 3 Refractive index matching experiments for sodium iodine solutions using: a) silica gel and b) Pyrex glass particles

References

•Abbas, M. A., & Crowe, C. T. (1987). Experimental study of the flow properties of a homogenous slurry near transitional reynolds numbers. International Journal of Multiphase Flow, 13(3), 357-364.
•Chen, R. C., & Kadambi, J. R. (1990). LDV measurements of solid-liquid slurry flow using refractive index matching technique. Particulate Science and Technology, 8(1-2), 97-109.
•Hadinoto, K., Jones, E. N., Yurteri, C., & Curtis, J. S. (2005). Reynolds number dependence of gas-phase turbulence in gas–particle flows. International Journal of Multiphase Flow, 31(4), 416-434.
•Lee, S. L., & Durst, F. (1982). On the motion of particles in turbulent duct flows. International Journal of Multiphase Flow, 8(2), 125-146.
•Pepple, M. A. (2010). Benchmark data and analysis of dilute turbulent fluid-particle flow in viscous and transitional regimes. University of Florida,
•Tavoularis, S. (2005). Measurement in fluid mechanics. New York, NY: Cambridge University Press.

UF UNIVERSITY of FLORIDA The Foundation for The Gator Nation
PIRE NSF
South East SEAGEP Alliance for Graduate Education and the Professoriate
PaSS

Polyhydroxy Fullerenes - Spectral Data Analysis

Angelina Georgieva[1], Vijay Pappu[2], Vijay Krishna[1], Ion Ghiviriga[3], Ben Koopman[4], Brij Moudgil[1], Pando Georgiev[2] and Panos Pardalos[2]

Particle Engineering Research Center[1], Center for Applied Optimization[2], Department of Chemistry-NMR Facility[3], Environmental Engineering Sciences[4], University of Florida, Gainesville, Florida 32611

Intellectual Motivation for the Research

Polyhydroxy fullerenes (PHF)'s estimation of number of hydroxyl groups is needed:

- **In order to understand electron scavenging properties of PHF.**
- **Since so far no successful example in the literature on elucidation of structure of PHF.**

Preparation Methods Used

- Modified Kitazawa (alkali) method (Li *et al.*, 1993)
- $C_{60}Br_{24}$ method (Schulz at al, 1996).

Characterization Methods Used

- FTIR
- XPS
- NMR
- TGA

Mathematical Methods Used

- GlobalSearch Algorithm

FTIR Spectra of PHF – Raw Data

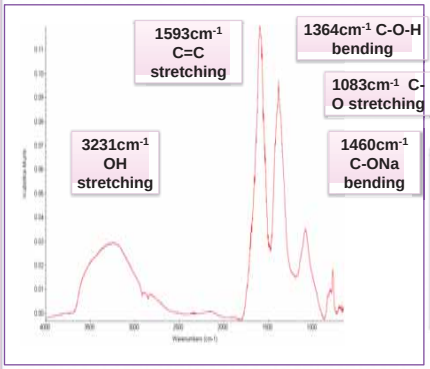

All Gaussian Curves of 3 FTIR Dataset – Inverted – Shown Essential Area 2000-800cm^{-1}

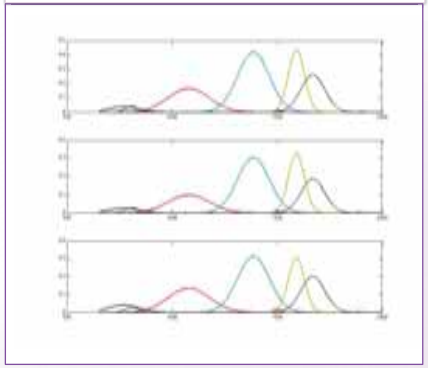

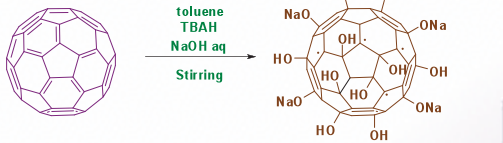

Industrial Relevance:

❖New mathematical approach for faster and more precise data analysis, applicable for quantitative evaluation of every spectral data in the chemical and biochemical industry

Our Approach: We developed algorithm for quantitative analysis of large amount of Fourier Transform Infrared Spectral Data in order to elucidate the structure of PHF

$C_{60}(OH)_{18-19}$

FTIR Spectra of Area of Individually Fitted Database Gave the Number of Hydroxyl Groups

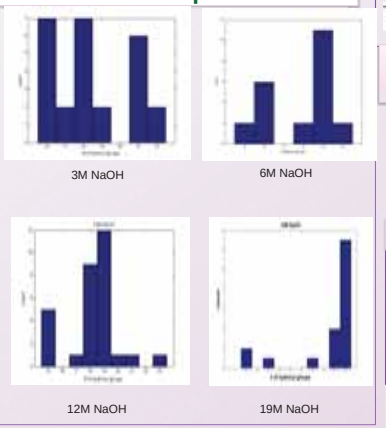

Cross - Validation

^{13}C NMR method

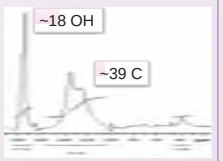

$C_{60}(OH)_{18}$

XPS method

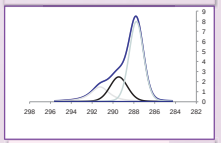

$C_{60}(OH)_{17}$

Mathematical Formulation

$$\min_{a,\mu,\sigma} \sum_{i=1}^{N}\sum_{k=1}^{p}\sum_{j=1}^{m} a_{jk}\exp(-(x_{ik}-\mu_{jk})^2/2\sigma_{jk}^{\ 2}) - y_{ik})^2$$

$$\sigma_{jk} = \sigma_{jr} \qquad \mu_{jk} = \mu_{jr} \qquad \mu_{jk}, \sigma_{jk}, a_{jk} \geq 0$$

N – number of observations in each dataset
p – number of peaks in the fitted curve
m – number of datasets for each experiment

j = 1,2,..m
r = 1,2,..p
k = 1,2,..p

Summary

- Developed was new mathematical algorithm to analyze spectral data more precisely and time efficiently.
- Cross-validated were different methods to find out the accuracy and precision of the different data analysis.

Future Work

- Analyze by better resolution XPS standard sample of PHF.
- Correlate experimental FTIR and NMR peaks with quantum theoretical predictions.
- Publish our results.

Acknowledgement: This material is based upon work supported by PERC, CNBS and CPaSS industry members.

Bioengineering Applications of Green Polymeric Nanoparticles: Tissue engineering

Sathish Ponnurangam[1], Grace D. O'Connell[1], Ponisseril Somasundaran[1] and Clark T. Hung[1] and V. Runkana[2]

[1]Columbia University, New York, [2]Tata Research Development and Design Center, India

Goals

- Nanotechnology for biomedical applications:
  - Nanogels & nanoparticles for actives extraction & release for tissue engineering and cosmetics
- One specific application: Articular human cartilages.

Broader Scope - Nanogels

- Controlled delivery of drug and nutrients
- Extraction of toxicants
- Diagnostic devices
- Sustained delivery of actives or fragrances in personal care
- Improving strength during setting of cement

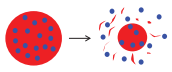

Drug Delivery

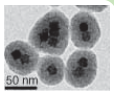

Diagnostic and contrasting agents

Tissue engineering

http://media.wiley.com/wires/WNAN/WNAN14/nfig006.jpg
http://www-cgi.uni-regensburg.de/Fakultaeten/Pharmazie/Pharmtech/php/en/forschung_tissue_6.php
http://www.uic.edu/labs/bpslab/drug_delivery.html

Introduction – Articular cartilage engineering

- Extracellular matrix elaborated during tissue culture in a hydrogel scaffold hinders further diffusion of nutrients, causing spatially inhomogeneous mechanical properties.

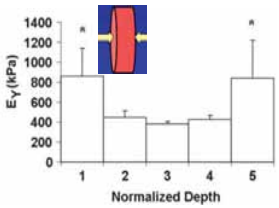

Bian, L., S. L. Angione, et al. (2009). Osteoarthritis and Cartilage 17(5): 677-685.

Objective is to use polymeric microgels (as delivery vehicle) embedded in a chondrocyte-seeded agarose scaffold for sustained delivery of essential nutrients to overcome hindered diffusion (Scheme 1).

Scheme 1: Hydrogel scaffolds with embedded microgels

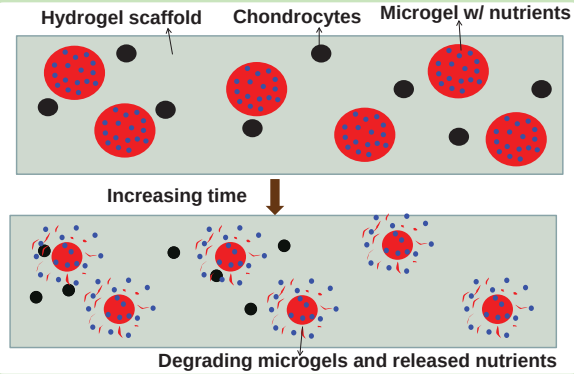

Synthesis of polymer and microgels

poly(Sebacic anhydride)

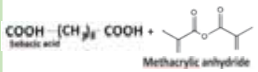

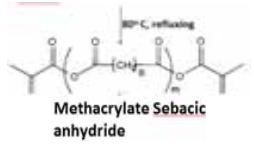

Synthesis of microgels

- Microgels synthesized using double emulsion (W/O/S) of water/methylene chloride/solid (bioactive) by solvent evaporation
- Sebacic anhydride polymer, PSA, dissolved in oil phase coated the internal solid phase (nutrients or bioactive molecules).
- Microgels encapsulated with ~20 mg of vitamin-C and glucose powders synthesized separately.

Scheme 2 Synthesis of microgels

W/O/W double emulsion method

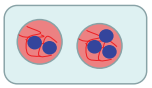

W/O/W double emulsion

Thermal crosslinking
Solvent Evaporation
(Methylene Chloride)

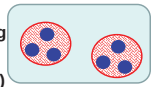

Nutrient encapsulated Polyanhydride microgels

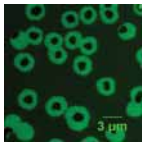

Confocal fluorescence image of microgels; Green shell- polymer, Black core- VitaminC

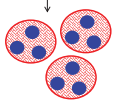

Centrifuge, washed and freeze dried

Release Kinetics & Mechanical properties

- Linear release of amitriptyline observed and ~ 28 % of drug was released by day 12 (see right).
- Microgels (with vitamin-C or glucose) were embedded in agarose hydrogel with 30M/mL chondrocytes. A gel without microgels served as the control.

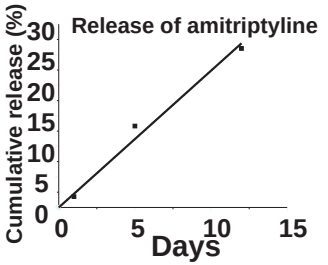

Release of amitriptyline drug from poly(sebacic anhydride)-based microgels.

Mechanical properties of engineered tissues

- Both the Young's (E_Y) (10% compressive strain) and dynamic moduli of microgel constructs greater than control (see below).

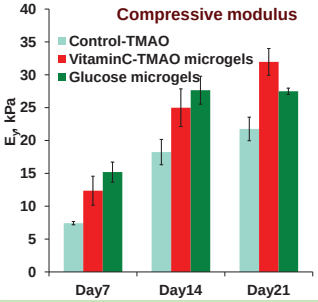

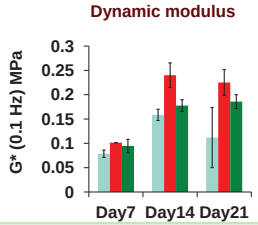

Raman analysis of articular cartilage tissue

- Raman spectra of engineered cartilage and native juvenile-bovine articular cartilage clearly demonstrated that the collagen content and the helical conformation was still lower in the engineered constructs (below).

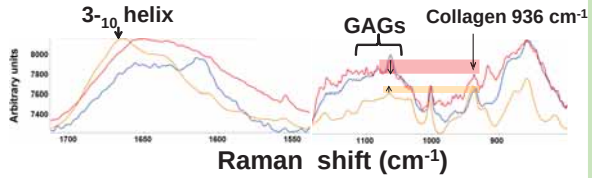

Conclusions and Future Work

- Sustained delivery of nutrients or drugs with no initial burst effect
- Cultured hydrogels with nutrient-loaded microgels improved mechanical properties.
- Collagen conformation and content of engineered tissue remain poor compared to native cartilage.
- Future aim is to improve collagen content relative to GAGs by delivering chondroitinase-ABC

Acknowledgements

This study is supported in part by CPaSS, NSF grant no. 0749481, NSF grants 0749461 and 0925232, Tata Research Development and Design Center (TRDDC), India, and NIH/NIAMS grants AR46568 and AR60361.

Investigation of surfactant- stratum corneum interactions: & Drying Stress Raman studies

Parag Purohit and P. Somasundaran
Columbia University New York, NY 10027
2012 Spring IAB - Feb 13 - 15

Rationale

- Stratum corneum (SC), outermost layer of epidermis
  - Consists primarily of proteins/lipids
  - Provides vital barrier function for the skin
- Cleanser formulations: Feel, appearance, delivery of actives
- Surfactants wash leads to - transient swelling and hyper-hydration followed by deswelling – dryness, cracking: driving force for further skin damage

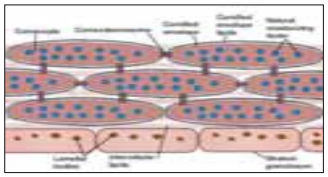

Current Objectives

- Drying stress study : Physical property to quantify the damage to stratum corneum (SC) on surfactant treatment
- Understand surfactant interactions with SC components : spectroscopic techniques such as Raman/ IR

Impact

- Industry specific : Knowledge generated will help design milder surfactant systems
- Broader Impact :
  - SC barrier function – **Pharmaceutical**
  - Thin film behavior – importance in **paints/ coatings/ Microelectronics/ renewable energy**

Materials/Methods:

- Stratum corneum separated from porcine skin

Dynamic Mechanical analyzer

- The specimen as a thin film is loaded between the clamps and kept under initial load (enough to straighten but not allowing significant stress)
- The change in force is measured as a function of drying time (or temperature) and converted to stress
- Stress-time plots for period of 6 -8 hours recorded

Raman spectroscopy

- Effect of surfactant binding to Stratum corneum: Protein and lipid structure

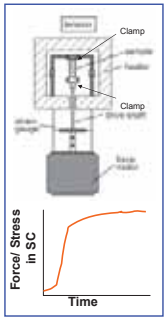

Drying stress: Single and mixed surfactant

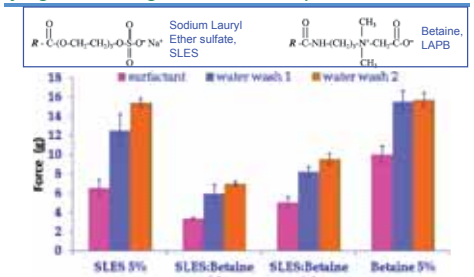

- Lower drying stress in SC observed by treatment with mixed surfactant system

Effect of surfactant treatment on skin: Raman study

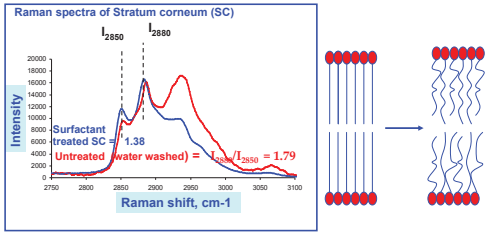

- Change in I_{2880}/I_{2850} ratio : Indication of lipid structural modifications
- Studies show lipid chain disorder on treatment with common surfactant systems

→ A technique to understand effect of surfactants on skin proteins/lipids

Effect of surfactant structure on Stratum corneum lipids – Drying stress and lipid rigidity

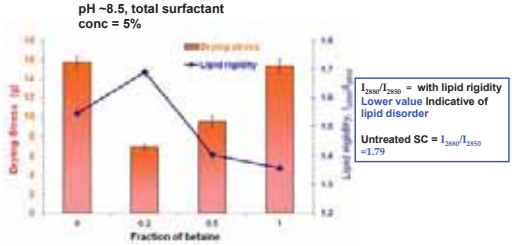

- Optimum performance (lower drying stress + better lipid rigidity) at 1:4 Betaine:SLES → **Minimum damage to SC lipids**

Lipid-Protein relative content by Raman analysis

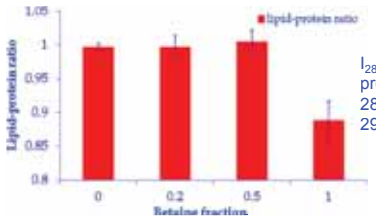

I_{2880}/I_{2930}: Lipid to protein ratio
2880: CH_2 str
2930: CH_3 Str

Lipid-protein ratio **decreases** in Betaine treated SC, indicating possible removal of lipids

Raman Mapping of SC: Methanol- chloroform (1:2) treatment

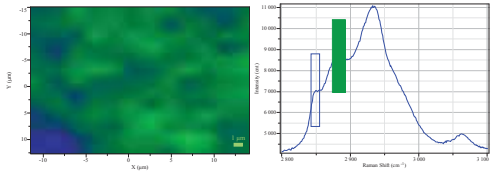

Ratio of I_{2880}/I_{2850} : Green region as 2880 (2872-2890) , and blue as 2850 (2840-2858)

- Relative lipid content in solvent treated stratum corneum The green region indicating ordered lipids, blue shows disordered lipids
- Mapping can give relative content of trans vs gauche conformation -> measure of lipid disorder

Summary

- **Drying stress increase** after surfactant treatment & water washes : indication of disruption of SC components
- **Lipid disorder** observed by Raman upon surfactant treatment
- **Lipid/Protein ratio decreases** after betaine treatment indicating removal of lipids
- A specific mixed surfactant ratio gives *optimum performance*

→ **drying stress and Raman as techniques to measure mildness of new surfactants**

Future work

- SEM of surfactant (ALS, SLES, betaine) treated SC samples: skin morphology studies
- Raman mapping studies to map the lipid disorder on SC
- Characterization of mixtures of SC lipids extracted as function of solvent/ surfactant treatment

Synthesis and Characterization of Biocompatible PHF-Chitosan Nanoparticles

Ailin Qin[1,3], Eric M. Bidinger[3], Vijay Krishna[3], Ben Koopman[2,3], Stephen Grobmyer[4] & Brij Moudgil[1,3]

[1]Department of Materials Science and Engineering, [2]Department of Environmental Engineering Science,
[3]Particle Engineering Research Center, [4]Department of Surgery, University of Florida, Gainesville, FL, 32611.

Industrial Relevance

- **Represents a new market with untapped revenue potential.**
  - **One million MRI screenings are needed per year for breast cancer.** (http://www.ncbi.nlm.nih.gov/pubmed/17036340)
  - **Projected cancer costs in 2020 to exceed 2010 costs by at least 27 percent. $16.5 billion was spent on treating breast cancer in 2010.** (http://www.esmo.org/no_cache/view-news.html?tx_ttnews[tt_news]=1031&tx_ttnews[backPid]=585&cHash=b58a05da78)
- **Pharmaceuticals**
  - **Safer multimodal product with imaging contrast and therapeutic capabilities**
  - **Photothermal release of actives (Transdermal patch with laser/radiofrequency irradiation)**
- **Other Markets**
  - **Photothermal release of nutrients and pesticides in agriculture sector**
  - **Photothermal release of nutrients and other actives in consumer product sector**
- **General Synthesis Method**
  - **Generalized to produce other biodegradable particles - nutrient loaded nanoparticles for cosmetics or agricultural applications**

Motivation & Objectives

- **Motivation**
  - **Develop multifunctional, biocompatible particles for imaging and targeted delivery in medical applications.**
- **Objectives**
  - **Synthesize PHF/Chitosan nanoparticles (optimize particle size, composition) to increase biocompatibility, retention time, and test their safety and therapeutic efficiency through *in vivo* studies.**
  - **Incorporate Gd atoms into the PHF in order to enhance MRI contrast.**

Methods

- **Synthesis procedures for nanoparticles (charge interactions)**

PHF + Chitosan ⟶ PHF-Chitosan nanoparticles
TPP + Chitosan ⟶ TPP-Chitosan nanoparticles
PHF + TPP + Chitosan ⟶ PHF-TPP-Chitosan nanoparticles

PHF + TPP + Chitosan ⟶ PHF-TPP-Chitosan

Model synthesis of PHF/Chitosan Nanoparticles, Gd will be incorporated inside of a PHF molecule

Results

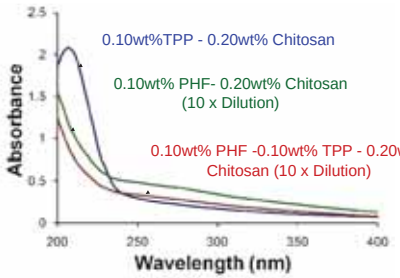

UV-Vis Absorbance of PHF/Chitosan Nanoparticles

(peaks move left)

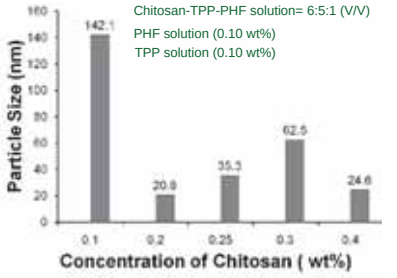

Particle Size of PHF-TPP-Chitosan nanoparticles

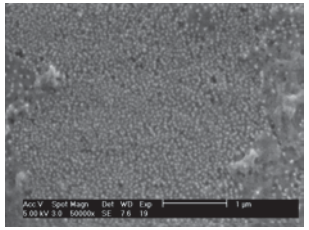

SEM image of Chitosan-PHF nanoparticles (0.25wt% chitosan)

Summary

- **PHF successfully encapsulated into Chitosan.**
- **Chitosan concentration influenced the Chitosan-PHF particle size.**
- **Particles with optimum size of PHF-Chitosan (less than 100nm) were synthesized.**

Future Work

- **Further optimize synthesis of PHF/Chitosan nanoparticles using chitosan of different molecular weights.**
- **Test Gd loaded nanoparticles for MRI contrast properties and photothermal therapy with laser/radiofrequency irradiation.**
- **Assess applicability for image-guided cancer therapy using photoacoustic imaging, MRI and photothermal ablation.**

Photothermal ablation of tumor with PHF/chitosan nanoparticles

Acknowledgement

This project is based upon work supported by the **Department of Defense**, **M.Q. Landenberger Foundation** and **PERC**.

UF UNIVERSITY of FLORIDA
The Foundation for The Gator Nation

iPass

Spring 2012 IAB Meeting – February 13-15, 2012

COLUMBIA UNIVERSITY
IN THE CITY OF NEW YORK

Deposition of Benefit Agents in Skin from Emulsion Cleansers upon Dilution

Jose Martinez Santiago, P. Somasundaran

Earth and Environmental Engineering Department, Columbia University, New York, 10027

Proposal objectives: To optimize deposition of beneficial agents on skin from rinse-off emulsion cleansers

Challenges: Polymer induced flocculation upon dilution is a complex process due to numerous factors, including; dilution factor, interaction between polymer and surfactant, pH, and the interaction of other ingredients in the cleanser.

Industrial Relevance: Obtaining a fundamental understanding of flocculation in emulsion cleansers upon dilution will lead to streamline-driven processes for defining the right composition of industrial formulations containing polymers, surfactants, and oils, and will help optimize deposition of beneficial agents in skin.

Broad Appeal: Fundamental models and theories developed will be helpful to product developers and formulators in industries where flocculation is a key process; such as personal care household, pharmaceuticals, mining technologies, etc.

Liquid body wash market

More consumers are using liquid body washes

There is an increased demand on deposition of *Benefit Agents* from rinse-off products

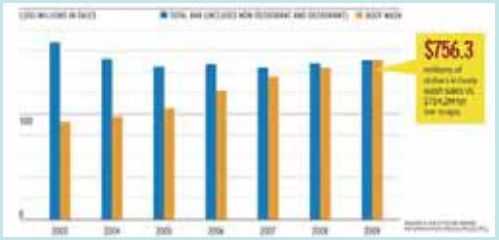

Factors affecting deposition of benefit agents upon dilution in surfactant-oil-polymer systems

Surfactant
Type
HLB
CMC

Oil
Type
Polarity
Melting Point

Polymer
Type
Molecular weight
Charge Density
Conformation

External factors

- Breakage of flocs due to shear
- Re-flocculation of broken flocs
- Floc Size
- Dilution factor
- Temperature

Deposition Mechanism upon foaming and dilution

- Electrostatic interaction
- Polymer-Surfactant Interaction
- Flocculation of oil droplets

COMPLEX SYSTEM, DIFFICULT TO PREDICT

Proposed hypothesis

1. Upon dilution, flocs are formed through polymer-surfactant interactions and flocculation of oil droplets

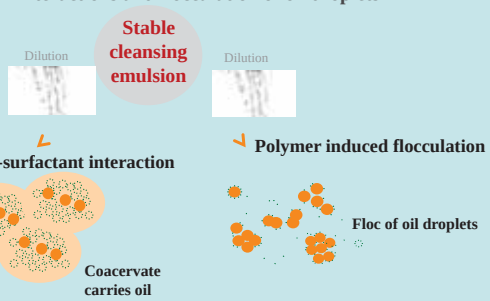

2. Floc size plays a key role in deposition

Studying the dynamics of flocculation upon dilution will help:

1. Elucidate mechanisms of deposition
2. Predict and optimize deposition

Proposed techniques for floc characterization: Optical microscopy, light scattering (floc size), zeta potential, fluorescence sp. etc.

Preliminary results

Effect of fatty acid on the floc size

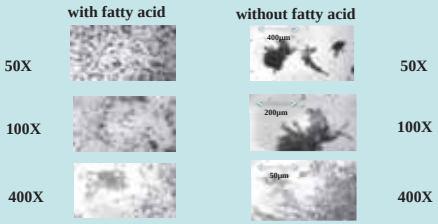

Fatty acids may *mask* the polymer and inhibit flocculation

Effect of fatty acid chain length on the floc size

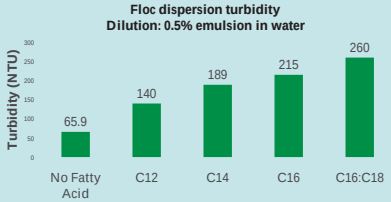

Flocculation inhibition increases with fatty acid chain length

Conclusions

- Deposition of beneficial agents from rinse-off cleansers in skin is challenging
- Floc size distribution is a key factor in the deposition process
- Deposition mechanisms need to be elucidated for emulsion systems
- Preliminary results showed that floc size distribution is significantly affected by pH and addition of fatty acids

Acknowledgement: This material is based upon work supported by the National Science Foundation under Grant No. 0749481 and by the CPaSS industry members.

UF UNIVERSITY of FLORIDA
The Foundation for The Gator Nation

CPaSS

COLUMBIA UNIVERSITY
IN THE CITY OF NEW YORK

Spring 2012 IAB Meeting – February 13-15, 2012

Vis-NIR Emitting Hydrothermal Quantum Dots for Biological and Photonic Applications

A. K. Saha, P. Sharma, H. Sohn, G. A. Walter, K. Powers and B. M. Moudgil

Particle Engineering and Research Center, Materials Science and Engineering, University of Florida, Gainesville, FL 32611

- ✓ Objective: To synthesize photostable, water dispersible, magnetic, visible and NIR emitting QDs with high quantum yield and precise size control.
- ✓ Challenges: Multifunctional QDs have varied biomedical and photonic applications, but rationally designing and developing these QDs is a challenging task.
- ✓ Intellectual Motivation: The multifunctional QDs can be used for diagnosis and therapy of cancer, and in developing high efficiency solar cells & gas sensors.
- ✓ Industrial Relevance: Hydrothermal synthesis of QDs use relatively inexpensive precursors and non-toxic surfactants compared to the traditional organometallic route.
- ✓ Broad Appeal: Applications include bio-imaging, solar cells, gas sensors, gene transfection etc.

Gene transfection

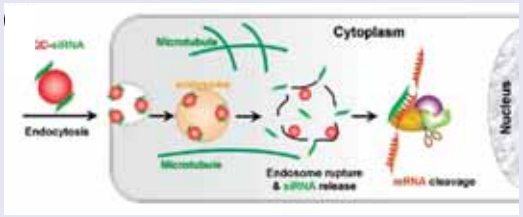

J. AM. CHEM. SOC. 2008 **130** 9006-9012

- Process of deliberately introducing genes (short sequences of nucleic acids) into cells.
- For treatment of cancer and hereditary diseases, caused by single gene defects.
- Gene transfection can be viral (e. g. herpes simplex virus, non-viral (e. g. cationic polymers) and physical (electroporation).
- Magnetic QDs can be used for efficient gene delivery.

Hydrothermal Synthesis

Batch Process

Flow Process

Bio-imaging

Fluorescent and Magnetic Bimodal QDs

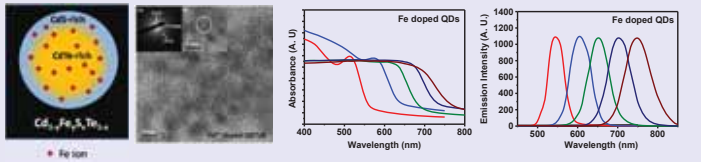

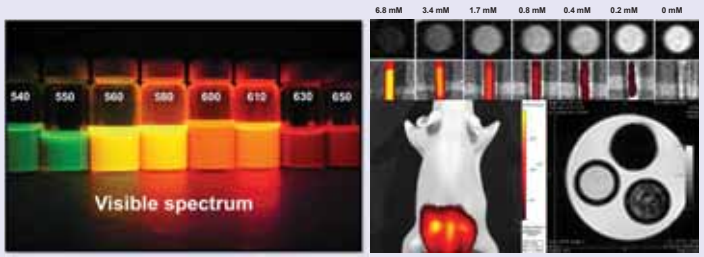

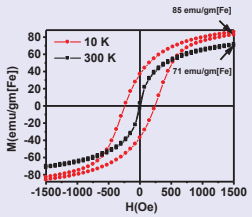

- Fluorescent and magnetic bimodal QDs developed.
- The QDs emit in the vis-NIR (560-740 nm) wavelength regime.
- The QY of the QDs vary within 9-67%.
- The QDs can be imaged using MRI.
- Core/shell QDs emitting upto 815 nm developed.
- The core/shell structure characterized using XPS, EDS and XRD.

Core/shell QDs

Solar cells

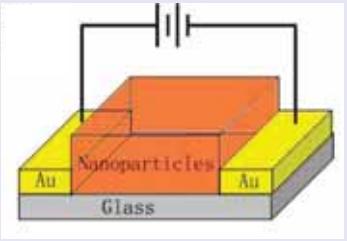

Chem. Mater. 2008 **20** 6906-6910

- Stacking of semiconductors atop one another forming mutijunction cells.
- Third generation solar cells having >30% power conversion efficiencies can be developed.

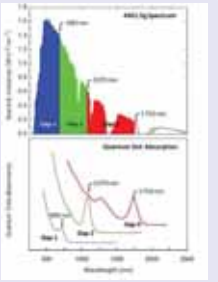

http://www.light.utoronto.ca/projects/photovoltaics

Solar spectrum showing optimal choices for individual bandgaps in a triple junction solar cell (top).

Advantages of Hydrothermal Synthesis

Parameters	Microemulsion	Organo-metallic	Hydrothermal
Water dispersibility	Yes	No	Yes
Quantum Yield	Low	High	High
Photostability	Moderate	Good	Good
Cost of precursor	Low	High	Low
Toxicity	Low	High	Low

Conclusions

- Developed magnetic and vis-NIR emitting QDs.
- The QDs are water dispersible, highly fluorescent and photostable.
- Characterized using TEM, XRD, XPS, optical spectroscopy, MRI.

Acknowledgements

- Particle Engineering Research Center (PERC)
- NSF-NIRT Grant # 0506560
- Materials Science and Engineering
- Major Analytical Instrumentation Center (MAIC)
- Interdisciplinary Center for Biotechnology Research (ICBR)

UF UNIVERSITY of FLORIDA
The Foundation for The Gator Nation

PASS

COLUMBIA UNIVERSITY IN THE CITY OF NEW YORK

Targeting of Polyhydroxy Fullerenes for Photothermal Applications

Neha Saxena[1,2], Vijay Krishna[2], Stephen Grobmyer[3], Ben Koopman[4], & Brij Moudgil[1,2]

[1]Dept. of Materials Science & Engineering, [2]Particle Engineering Research Center, [3]Dept. of Surgery, [4]Environmental Engineering Sciences, University of Florida: Gainesville, FL 32611

Industrial Relevance: Pharmaceuticals; Imaging

Broader Impacts: Disinfection; Photoacoustic imaging for trace mineral detection

Goal

Conjugate polyhydroxy fullerenes to targeting agents for site-specific delivery

Polyhydroxy Fullerene (PHF):

$C_{60}(OH)_{22-24}$

Antibody:

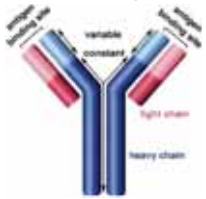

Objectives:

- Attach PHF to antibodies
- Retain photothermal and targeting capabilities

Research Approach & Novelty

Conventional Approach to Conjugation: many steps; tricky chemistry

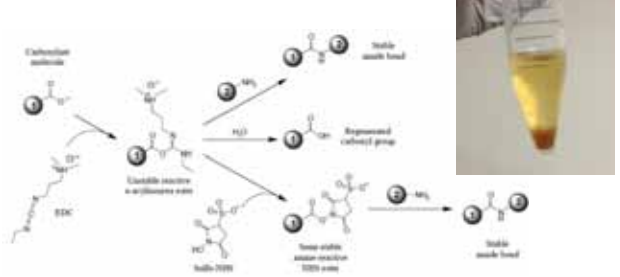

Pros: covalent bonding; conjugates tough as nails
Cons: Aggregation; active sites hidden

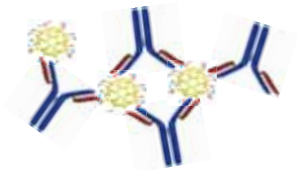

Aggregates due to PHF reacting with more than one antibody

- Fewer available active sites
- Decreased targeting

Proposed One-Step Approach to Conjugation: mix PHF with antibody

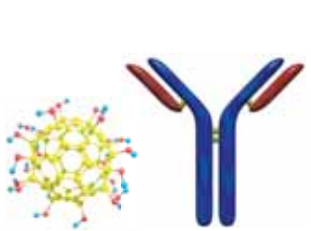

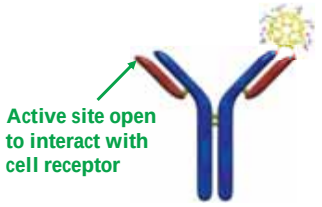

The hydroxyl groups on the PHF react with amine groups present on specific amino acids

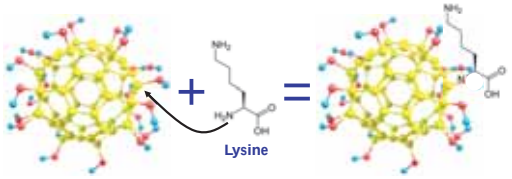

Judicious simple mixing results in fewer aggregates. Mass spectrometry analyses are in progress to evaluate the conjugation efficiency.

Preliminary Results: Photothermal Effects of PHF

Heating/Cooling Profile of Conjugates

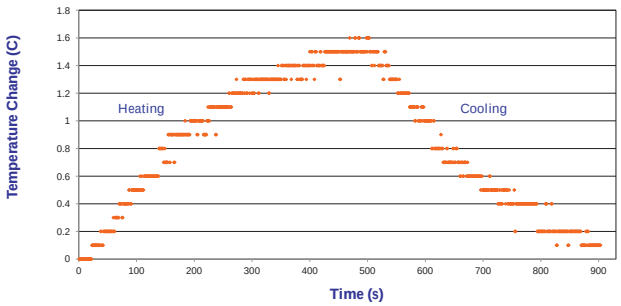

- 785 nm laser at ~500 mW
- 10 PHF molecules per 1 antibody

Heating Rates as a Function of PHF Concentration

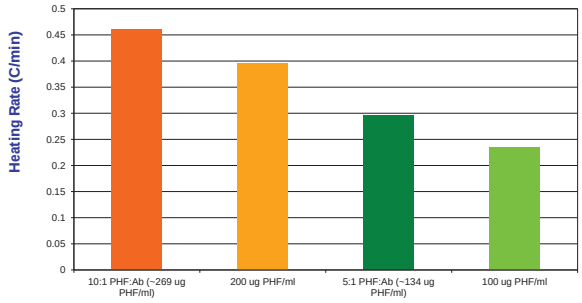

- Heating rates maintained for PHF-Ab conjugates

Summary

- PHF seems to heat just as well when conjugated to antibodies as it does in solution by itself

Future Work

- Determine how many PHF molecules are conjugated to one antibody and where they are present on the antibodies using mass spetrometry
- Optimize conjugation protocol to minimize aggregation
- Determine the targeting efficacy of the PHF-Ab conjugates
- Perform *in vivo* studies to target breast cancer tumors

Acknowledgements

Dept. of Defense, BCRP Concept Award (W81XWH-10-1-0805); M. Q. Landenberger Foundation; Particle Engineering Research Center; Major Analytical Instrumentation Center; Water Reclamation & Reuse Laboratory

UF UNIVERSITY of FLORIDA
The Foundation for The Gator Nation

IAB-I/UCRC PaSS February 14, 2012

COLUMBIA UNIVERSITY IN THE CITY OF NEW YORK

Development of the Greenness Index

Yang Shen[1], Chi Lo[1], Jun Wu[1],

D. R. Nagaraj[2], Raymond Farinato[2], P. Somasundaran[1]

[1]*Earth and Environmental Engineering, Columbia University, New York, NY 10027*

[2]*Cytec Industries, Stamford, CT 06904*

Spring 2012 IAB Meeting – February 13-15, 2012

Challenges

Holistic Green or Greener Processing Practices are needed

Introduction

Greenness needs to be defined and evaluated before implementing holistic Green or Greener processing practices.

However,

- *No widely accepted definition*
- *Each industry has its own unique attributes, and thus a specific definition*
- *Each industry is composed of various components, and they should all be evaluated systematically*

Goal

To develop a **Greenness Index** Tool in which

- *Reagent is the starting point for the definition and evaluation*
- *Other factors, such as water, energy, cost, could be evaluated as affiliated to reagent*

The **Greenness Index** will be capable of being:

- *Used to define and evaluate Greenness*
- *Applied to a specific industry by incorporating industry-specific characteristics*

Significance

Intellectual Motivation:

a first tool to define and evaluate the Greenness comprehensively using multi-disciplines

Industrial Relevance:

the Greenness Index will help companies evaluate their processing practice and make improvements to achieve sustainability goal with lower costs

Broad Appeal:

the Greenness Index will be applicable to various industries by incorporating industry-specific characteristics

Roadmap

1. Create a comprehensive list of criteria/metrics

(describing the characteristics of reagents that can define and evaluate its Greenness)

- ***Conduct LCA (Life Cycle Analysis) in the following aspects:***
  - *Social: labor intensity, safety…*
  - *Health: toxicity, carcinogenicity…*
  - *Environment: water pollution, green house gas emissions…*
  - *Companies: cost, performance…*

↓

2. Collect the permissible limit for each criterion/metric

- ***From EPA, OSHA, ACC, Clean Water Act…***

↓

3. Collect the information on the behavior of the reagent corresponding to each criterion/metric

- ***From literature***
- ***Develop methods to study the reagent***

↓

4. Assign a score for each criterion/metric

(by comparing the permissible limit and the behavior of the reagent)

- ***Use standard algorithms***

↓

5. Acquire the overall Greenness Index of the reagent by multiplying weighting factors to the scores

- ***Different companies could achieve different Greenness Indices for the same reagent due to the different weighting factors***

A simplified LCA *(life cycle analysis)* for reagent:

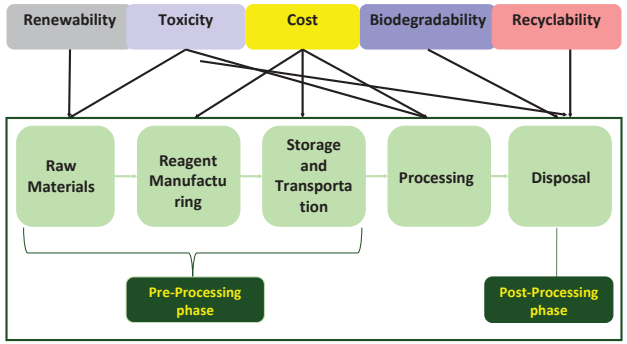

Selected properties of reagents will be evaluated during simplified LCA

Result

1. Divide the list of criteria/metrics into groups.
2. Assign a individual score for each criterion/metric in each group using various algorithms, for example:

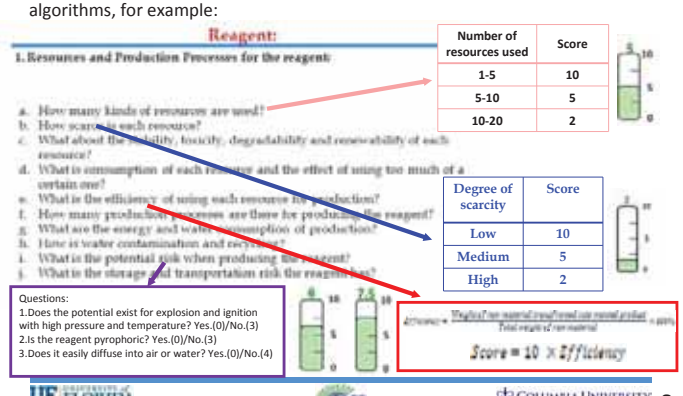

Result

3. Apply the weighting factor, *f*, to the individual score to get the group score and then the Greenness Index:

$$\text{Group Score} = \sum f_{individual} \times \text{individual score}$$

$$\text{Greenness Index} = \sum f_{group} \times \text{group score}$$

4. Present the Greenness Index in different ways:

(1) A value showing just the final Greenness Index, for example,

Greenness Index = 82.00/100.00

(2) Area Diagram
(group score can be seen):

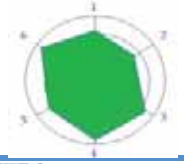

(3) Detailed Diagram
(individual score can be seen):

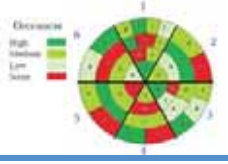

Silica Supported Nanocrystalline Manganese Oxides For Biomedical And Industrial Applications

H. Sohn[1], P. Sharma[1], J. Sun[1], A. Saha[1], C. Baligand[3], H. Zeng[2], B. M. Moudgil[1] and G. A. Walter*[3]

Particle Engineering Research Center, Materials Science and Engineering [1], McKnight Brain Institute[2], UF and Physiology and Functional Genomics[3], UF; Gainesville

Objectives: Synthesis of silica supported nanocrystalline manganese oxides

Challenges: Deposition of manganese oxides on the surface of silica nanoparticles while maintaining morphology and obtaining crystallinity.

Intellectual Motivation: To develop silica supported crystalline manganese oxides nano-composites

Industrial Relevance: Manganese oxides, 1) Cleaning waste gases from petroleum refineries and chemical manufacturing industries 2) Sequestration of heavy metals 3) Battery 4) Catalysis 5) Sensor 6)MRI contrast agent

Broad Appeal: Silica supported manganese oxides nanoparticles have potential applications in industrial, environment and biomedical research.

Background: *Industrial & Biomedical applications of MnO_x*

- Manganese oxides are one of the strongest oxidants that in redox reactions.
- Deposit on the surface of silica nanoparticles (support medium) leads to reduction of diffusion path and enlargement of contact area.

Applications:

The crystal structures of birnessite

Mn(IV)-Mn(III)

- Negative charges arise in Mn(IV) oxide minerals because of the presence of some Mn(III).
- Protons or alkali, alkaline earth, and transition metal cations are sorbed to compensate the negative charge.

Nelson & Lion 2003

- Sequestration on heavy metals (removal of Cr, Pu, U, by biogenic MnO)
- Energy Storage (Dry cell battery, Ultracapacitor)
- Catalysis (CO oxidation, Ozone Decomposition)
- Bioimaging (MRI contrast agent)

Nano Res (2009) 2: 54 60

Silica-manganese oxides as MRI contrast agent

- Advantages of SiO_2 Nanoparticles:
  - High surface-to-volume ratio
  - Non-toxic and biocompatible
  - Surface modification for bioconjugation and targeting
- Pros and cons of Manganese oxide Nanoparticles:
  - Mn-chelated Teslascan (a clinically approved contrast agent)
  - Poor in-vivo stability and toxicity
  - SiO_2-Manganese oxide hybrids : incorporates benefits from both SiO_2 and MnOx while mitigating limitaions

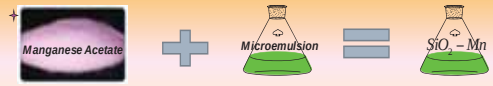

http://www.avachemicals.net/manganese-acetate-tetrahydrate.html

Synthesis and Characterization of Silica Supported Nanocrystalline Manganese Oxides

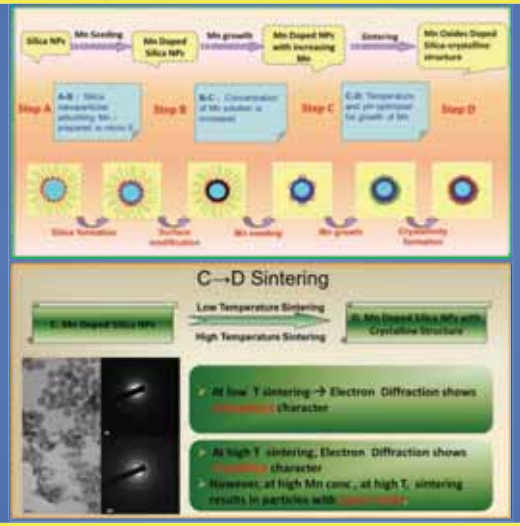

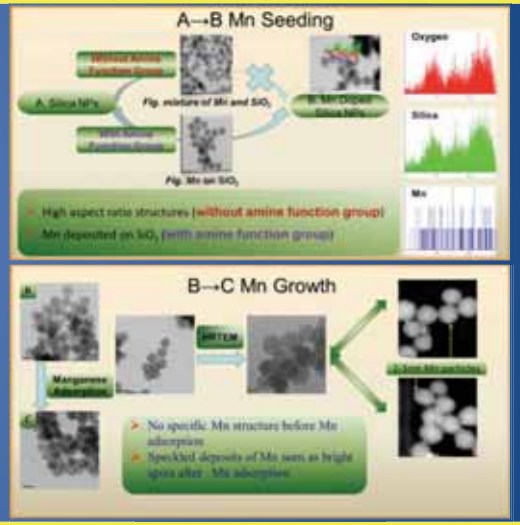

Mn Doped Silica Nanoparticles as MRI Contrast Agent

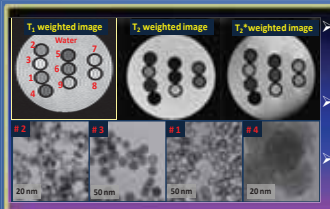

- Preliminary MR measurements demonstrate the ability of generating T_1, T_2 and T_2* contrast
- Top panel shows the representative T_1, T_2 and T_2* weighted images
- Bottom panel shows representaive TEM pictures (#5-8 $MnCl_2$; # 9 H_2O)

Summary and Future Plan

- Synthesis and characterization of SiO_2-MNO_x completed

Future work:

- Exploration of particle potential as nano-scavenger
- Evaluation as high field (17T) MRI contrast agent

Acknowledgements:

We thank NSF (EEC-0506560), The NIH, PERC and the National High Magnetic Field Laboratory, AMRIS - McKnight Brain Institute

Is TiO_2 a Visible Light Photocatalyst?

Abhinav Thakur[1], Wei Bai[2], Vijay Krishna[1], Ben Koopman[2], Brij Moudgil[1]
[1]Particle Engineering Research Center, [2]Department of Environmental Engineering Sciences, University of Florida, Gainesville

At the Macro Scale

- Rutile phase of TiO_2 is used as a UV protectant in sunscreens.
- The anatase phase of TiO_2 shows photo catalytic activity in UV-light at the macro scale.

Hypothesis: Both Rutile and Anatase phases of TiO_2 are photo active at the nano scale when exposed to visible light.

Why TiO_2?

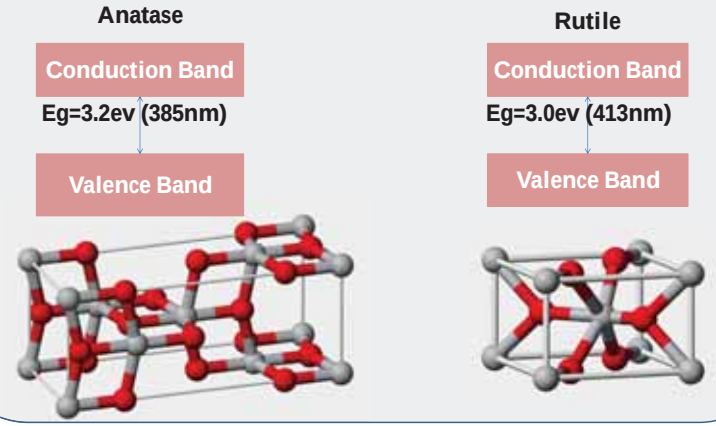

Industrial Relevance

- TiO_2 photocatalytic coatings can be used in air filters for emission reduction and air purification.
- Self cleaning and sterile surfaces can be prepared by coating them with TiO_2 coatings.

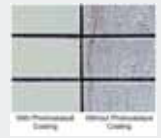

Harvesting Nanotechnology for better Photo Catalytic Performance

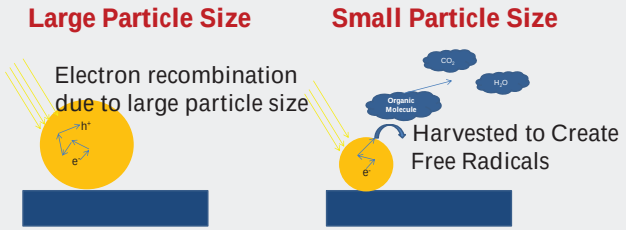

- The carrier diffusion length needed by an electron – hole pair is less in case of nano-sized particles. Hence the amount of carriers harvested are much more than with larger particle sizes.

Results

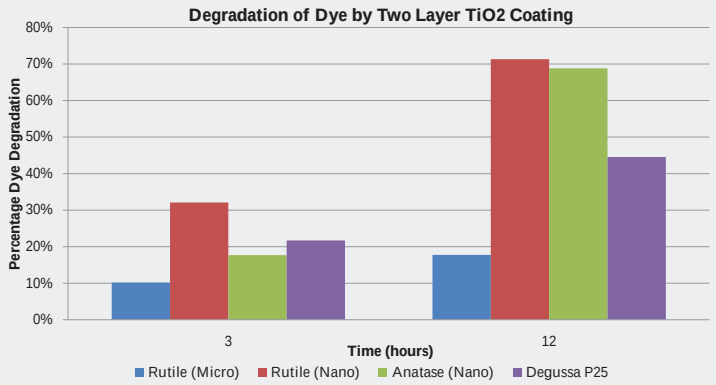

The dye degradation data clearly suggests that Rutile and Anatase are both much more photo-active at the nano scale.

Future Work

- Various formulations of anatase and rutile TiO_2 will be experimented with to get an optimal mixture.
- Bacteria and microorganisms could be tested for the visible light photo catalytic activity of TiO_2

Acknowledgements

This work was carried out with funding from NSF-AIR (1127830) for Particle Science & Technology.

The effect of lipid removal on the mechanical properties of Stratum Corneum

P. Somasundaran/Annamaria Vilinska
Columbia University

Center for Particulate & Surfactant Systems (CPaSS)
Spring 2012 IAB Meeting
University of Florida, Gainesville, FL
February 13-15, 2012

Introduction

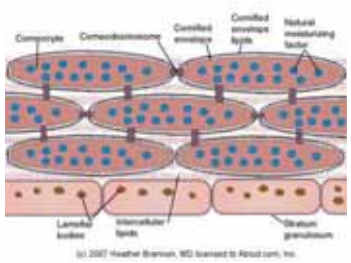

The intercellular lipids in Stratum Corneum are a well-balanced system of
- water
- cholesterol
- cholesterol esters
- ceramides
- fatty acids

Under ideal composition and pH conditions, the system is in a **liquid crystal form**, ensuring the proper function of skin barrier.

Surfactants used in personal care products can

- **remove the surface lipids from the skin**
- bind to proteins
- cause swelling, eventually protein dissolution

→ skin irritation, tightness, dryness, itching

Goal

Identify the lipids released from the skin and **quantify the responses** of the removal in the form of irritation, surface roughness and skin tightness.

If the compounds with the highest responses are identified, some actions can be taken to restore the skin condition or to prevent the release in the first place.

Materials and Methods

Lipid extraction from SC: Skin samples were soaked in Acetone, Methanol, Chloroform and Chloroform-Methanol for 10 minutes.

Measure the mechanical properties of lipid-extracted skin: drying stress measurements may reflect the skin tightness experienced after washing. Dry skin samples ere wetted in tap water for 30 minutes and the developing tension during drying was measured.

Identification of the changes within the skin after lipid extraction: estimated the lipid removal with Raman spectroscopy by lipid to protein peak comparison.

Important Results

Drying stress of SC after 10 minutes treatment in acetone – the effect of water wash

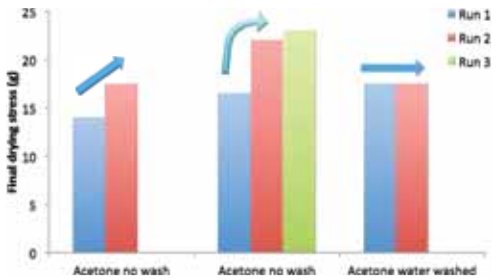

The drying stress increased with subsequent washing - possible lipid release during washing.

Important Results

Mean drying stress of SC treated with solvents for 10 min

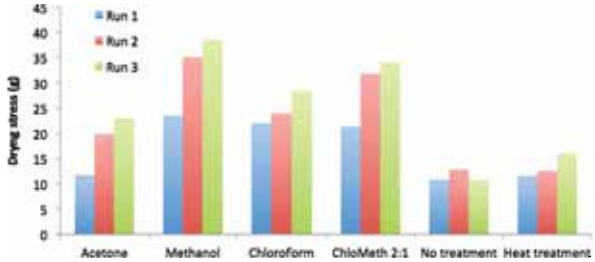

All solvent treatments increased the drying stress when compared with untreated skin. Solvents with the highest potential of lipid removal (Methanol and Chloroform Methanol 2:1) amplified the drying stress the most.

Raman spectroscopy of solvent treated SC

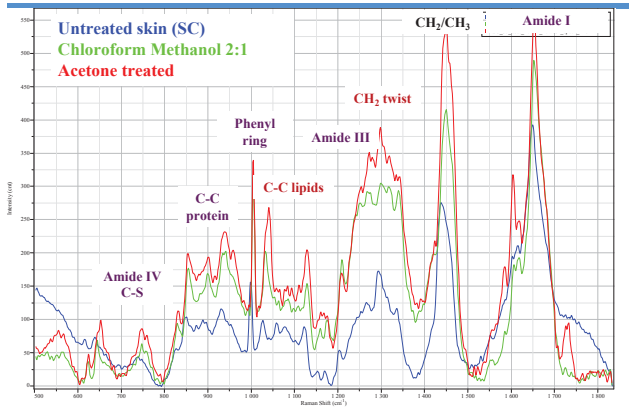

Comparison of certain Lipid and Protein peaks may indicate changes in lipid content.

Results

Lipid/Protein peak intensity ratio of solvent treated skin

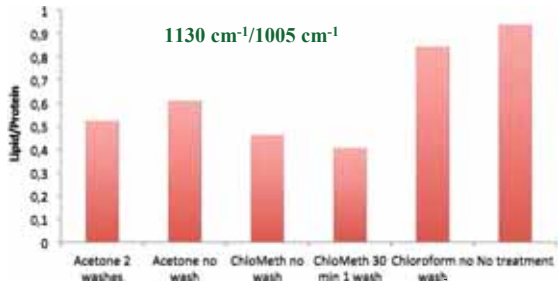

Untreated skin has the highest lipid content and lowest drying stress, while the Chloroform Methanol treated samples have very low lipid content and elevated drying stress results. Lipid content ↓ => Drying stress ↑

Summary

The stress developed during drying is a function of solvent treatment and lipid solubilizing capacity of the particular solvent system.
Drying stress development:

No treatment ▪ Heat treatment < Acetone < Chloroform < Methanol ▪ ChloroformMethanol 2:1

Non-polar solvents yielded a lower drying tension response compared to systems containing a polar protic solvent. The intensity of drying tension is in good agreement with the extent of lipid removal.

Future plans:

- Lipid identification (HPLC-MS)
- Lipid mapping studies
- Fluorescence imaging

Acknowledgment

This material is based upon work supported by the National Science Foundation under Grant No. 0749481 and by the CPaSS industry members

The Effect of Indoor Light Luminosity on Photocatalysis

Laurence Vincent[1,2], Wei Bai[1,3], Ben Koopman[1,3], Vijay Krishna[3], and Brij Moudgi[3,4]
[1]Department of Environmental Engineering, [2]Undergraduate Scholars Program, [3]Particle Engineering Research Center,
[4]Department of Materials Science and Engineering, University of Florida, Gainesville, FL

Introduction

The goal of this project is to understand the effects of light luminosity on photocatalysis in a realistic indoor environment. To do this, a dye-degradation experiment was carried out using TiO_2 and Procion red dye. Ceramic tiles covered in TiO_2 and the dye were exposed to light for 12 hours, and the degradation was measured to note the change as a function of light luminosity. The luminosities were chosen to emulate a realistic office environment.

Industry Relevance

This application of photocatalysis can be used for all of the following:

- **Removal of VOCs**
- **Odor control & air sanitizer**
- **Add-in for presently used household disinfectants**
- **Controlled release of perfumes and other actives**
- **Antimicrobial coatings**

Materials and Methods

The backing to the dye-degradation experiments were white tiles. The TiO_2 layer was created by first applying TiO_2 particles of diameter 5nm in the rutile form, and then applying TiO_2 in the anatase form with a particle diameter of 7nm. Once this layer dried, the tiles were then coated with dye. The environment's luminosity was detected using a global radiometer, and the exposure time was 12 hours, with measurements taken at 0, 1, 3, 6, and 12 hours. Degradation was measured through visible light spectrophotometry, measuring the absorbance of the tile at each time.

Data and Results

The two data sets were compared at the observed absorbance peak of 519nm. The results are as follows and are graphed below:

- **Luminosity of 1.9 W/m²:**
  - **55% degradation after 6 hours**
  - **67% degradation after 12 hours**
- **Luminosity of 5.0W/m²**
  - **75% degradation after 6 hours**
  - **81% degradation after 12 hours**

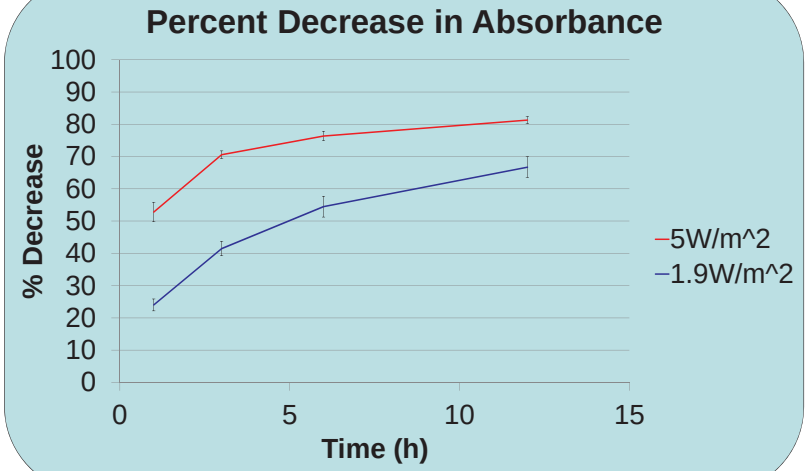

Acknowledgement: This material is based upon work supported by the National Science Foundation under Grant No. 0749481, NSF-AIR Grant No. 1127830, CNBS, and by the CPaSS industry members.